PN-ACF-774
102

ANNUAL REPORT

COVERING PERIOD NOVEMBER 15, 1996 to NOVEMBER 15,1997

SUBMITTED TO HUMAN CAPACITY DEVELOPMENT
BUREAU FOR GLOBAL PROGRAMS, FIELD SUPPORT AND RESEARCH
U S AGENCY FOR INTERNATIONAL DEVELOPMENT

"HIGHLY EFFICIENT METHODS FOR SEA-WATER DISTILLATION
UTILIZING SOLAR ENERGY"

PRINCIPAL INVESTIGATOR DR A I KUDISH
GRANTEE INSTITUTION BEN-GURION UNIVERSITY OF THE NEGEV (BGU, ISRAEL)

COLLABORATOR DR G MINK
INSTITUTION THE HUNGARIAN ACADEMY OF SCIENCES (HUNGARY)

PROJECT NUMBER C15-050
GRANT NUMBER TA-MOU-95C15-050

USAID GRANT PROJECT OFFICER DR DAVID MULENEX

PROJECT DURATION NOVEMBER 15, 1995 to NOVEMBER 14, 1998

II TABLE OF CONTENTS

I	TITLE PAGE	
II	TABLE OF CONTENTS	1
III	EXECUTIVE SUMMARY	2
IV	SECTION I	4
	Note on Publications	4
	A Research Objectives	4
	B Research Accomplishments	4
	C Scientific Impact of Collaboration	4
	D Description of Project Impact	5
	E Strengthening of Developing Country Institutions	5
	F Future Work	6
V	SECTION II	7
	A Managerial Issues	7
	B Budget	7
	C Special Concerns	7
	D Collaboration, Travel, Training and Publications	7
	E Request for USAID or BOSTID Actions	8
APPENDICES		9

A Publication Reprints

I G Mink, M M Aboabboud, L Horvath, E G Evseev and A I Kudish, Design and performance of an air-blown, multiple-effect solar still with thermal energy recycle *Proc Int'l Solar Energy Society Conference, Solar World Congress 1997,* **6**, 135-144, Taejon, Korea, Aug 1997

II A I Kudish, E G Evseev, M M Aboabboud, L Horvath and G Mink, Heat transfer processes in an air-blown, multiple-effect solar still with thermal energy recycle *Proc Int'l Solar Energy Society Conference, Solar World Congress 1997,* **6**, 158-167, Taejon, Korea, Aug 1997

III DESIGN PARAMETERS, PERFORMANCE TESTING AND ANALYSIS OF A DOUBLE-GLAZED, AIR-BLOWN SOLAR STILL WITH THERMAL ENERGY RECYCLE Submitted to *Solar Energy* (28 10 97)

III EXECUTIVE SUMMARY

The consumption of water unfit for drinking, due to pathogens or salinity, is a major worldwide health hazard and sufficient cause to undertake projects that recover water and make it suitable for human consumption The extent of the worldwide health hazard is manifested by the following statistics there are approximately 5 billion cases of water-borne sickness per year resulting in about 1 million deaths per year , most of these amongst children In addition, if the latter part of the 20th Century can be characterized as one that the scarcity of of oil was and still is a casus belli, than it is reasonable to state that the casus belli in the 21^{rst} Century will be the scarcity of water In fact, the success of the peace treaties now in effect and in the making in the Middle East will depend to a significant degree on the availability of water for all countries concerned Solar desalination can be an an important source for water in this region, which is primarily composed of semi-arid and desert lands and has an abundance of solar radiation

During the time interval covered by this report, the work performed at both institutions has progressed within the guidelines presented in the original proposal TIME CHART, except for a delay in the incorporation of nocturnal heating experiments These will performed during the third year of the program Both groups proceeded with the design, construction and testing of 2 m^2 solar stills The RLIC group replaced the 3 mm thick glass double glazing with a 10 mm thick double-walled polycarbonate sheet The theoretical work, both at BGU and RLIC, has been focused on the solution of the mathematical model of the still The two groups have approached the solution by different routes, since the model cannot be solved analytically The two models are now in the process of being validated by experimental data The results of the second year's efforts are documented in the Appendix, viz , the Publication Reprints

During the third year of the program the BGU group will test a third generation 2 m^2 solar still fabricated from stainless steel This still is similar in design to that of the second generation still which was fabricated from galvanized iron with some modifications

These modifications were applied to the previous design as a result of the experience gained from the testing of its predecessor It is anticipated that the large solar still system to be constructed during this year will be based on this design The RLIC group plan to begin the construction and testing of an innovative variation of their original module constructed, in part, from polymeric materials The intention of this module, which is presently in the design stage, is to eliminate the double tray required by the original still module and to construct it from non-corrosive materials

Dr Kudish and Dr Mink applied their second year's travel allowance, with the permission of Dr David Mulenex the USAID Grant Project Officer, toward the cost of attending and participating in the International Solar Energy Society's 1997 Solar World Congress, which took place in Taejon, Korea in August 1997 They each presented a paper describing the work being performed under this joint research program and utilized the congress venue to discuss their joint research program between themselves and with other interested participants attending the congress

IV SECTION I

Note on Publications

The close collaboration between the two senior investigators in the preparation of the the grant proposal resulted in their collaboration in the preparation of two papers describing the results obtained during the second year of the research program These papers were presented at the biennial conference of the International Solar Energy Society (ISES) 1997 ISES Solar World Congress, SOLAR MEANS BUSINESS, which took place in Taejon Science Town, Taejon, Korea from August 24-30, 1997 The complete manuscripts were published in the conference proceedings and reprints of the manuscripts are included in the Appendix

A third manuscript describing the work performed on the second generation solar still, utilizing the new solar simulator and replacing the double glazing consisting of two 3 mm glass panes with a single sheet of Qualex (a 10 mm thick double-walled polycarbonate sheet), has been submitted to *Solar Energy* (28 10 97) A copy of this manuscript is also included in the Appendix

A Research Objectives

The research objectives of this project remain essentially unchanged, viz , to achieve, by a joint research effort, a solar still design that is capable of producing water at a cost competitive with the local alternatives

The specific research objectives remain as stated previously and are as follows

To optimize the heat and mass transfer processes of the thermal recycle, thereby improving system efficiency and productivity (viz , enhance the fresh water yield per unit area)

To validate the mathematical models developed to describe the system, which will facilitate both in the optimization of the process and system scale-up

To develop hybrid systems which utilize (external on-site) waste energy for nocturnal heating (distillation), thereby approaching 24 hour per day system operation

To simplify the system design in order to minimize the level of technical skills required for system maintenance

To arrive at a design(s) that is amenable to the construction of a high capacity solar desalination plant, preferably a modular still design

B Research Accomplishments

The research accomplishments during the second year of this joint research program are attested by the three reprints/preprints attached to this report in the Appendix

C Scientific Impact of Collaboration

There has been a constant exchange of information between the collaborating scientists via email and fax This is especially true with regard to the preparation of the abovementioned manuscripts The two PI's met in August 1997 during the ISES 97, Solar World Congress in Taejon, Korea, during which time they discussed the technical, theoretical and managerial aspects of the research program in detail The PI's at both institutions are directly involved in all aspects of the study, i e , both experimental and theoretical Dr E Evseev of the BGU and Messrs L Horvath and M M Abboabboud of the RLIC have been intimately involved in the development of the mathematical model of the solar still and consequently have become quite proficient in their understanding of the heat transfer processes involved in the system The two groups have developed

independently mathematical models to describe the heat and mass transfer processes occurring in the proposed solar still design Both models utilize non-linear differential equations to describe the system under transient and steady state conditions The major difference is their approach to the solution of the non-linear differential equations describing the system The RLIC group utilizes an empirical exponential equation between the enthalpy and and temperature of the air/water vapor stream to convert the non-linear differential equations, which do not possess analytical solutions, into differential equations with simple exponential coefficients The BGU group applies numerical integration to solve the non-linear differential equations

D Description of Project Impact

It is too early in the research and development phase of this study to relate to this question The significance of this research project is obvious in that potable water is a commodity that is becoming scarce and has been a source of conflict between nations throughout history If the latter part of the 20th Century can be characterized as one that the scarcity of of oil was and still is a casus belli than it is reasonable to state that the casus belli in the 21rst Century will be the scarcity of water In fact, the success of the peace treaties now in effect and in the making in the Middle East will depend to a significant degree on the availability of water for all countries concerned Solar desalination can be an an important source for water in this region, which is primarily composed of semi-arid and desert lands and has an abundance of solar radiation In addition, there are approximately 5 billion cases of water-borne sickness per year resulting in about 1 million deaths per year , most of these amongst children

E Strengthening of Developing Country Institutions

During the past year both infrastructure and technical capabilities have been developed at RLIC as a result of this research program, thereby enhancing its research and development programs The following items has been purchased two HP DeskJet color printers, computer programs for mathematical analysis, conductivity meter for measuring quality of distillate, tools and materials for construction of solar stills and new solar simulator

Dr Mink presented a lecture entitled "Energy Saving Solar Stills ISRAELI-HUNGARIAN USAID PROJECT" on February 28, 1997 at a regular session of the Committee of Environment Protection of the Hungarian Academy of Sciences The paper was coauthored by Mink, Aboabboud, Horvath and Kudish

Mr M M Aboabboud submitted his PhD dissertation (146 pp including table and figures with 101 references) entitled "DESIGN AND INVESTIGATION OF A NEW, AIR-BLOWN SOLAR STILL WITH INTERNAL ENERGY RECYCLE" Mr Aboabboud is very grateful to Dr Kudish for his support, ideas and advice during the course of his dissertation work, which overlapped with the first 18 months of this USAID program

Two lectures were presented by the Hungarian group at the regular scientific seminar of the RLIC

i Dr Mink- "SOLAR DESALINATION ISRAELI-HUNGARIAN USAID PROJECT", coauthored by Mink, Horvath, Aboabboud Evseev and Kudish

ii Mr Horvath- "A NEW TYPE SOLAR CONCENTRATOR TO ACHIEVE INDUSTRIAL TEMPERATURES", coauthored by Horvath and Mink

Dr Mink presented a lecture entitled "ACHIEVEMENT AND TRENDS IN SOLAR TECHNOLOGIES" on

May 7, 1997 for a retraining course for army officers at the Regional Environmental Safety Center for the Army in Budapest

Dr Kudish and Dr Mink applied their second year's travel allowance, with the permission of Dr David Mulenex the USAID Grant Project Officer, toward the cost of attending and participating in the International Solar Energy Society's 1997 Solar World Congress, which took place in Taejon, Korea in August 1997 They each presented a paper describing the work being performed under this joint research program In addition, Mr Horvath was also able to attend this congress, with partial Hungarian travel support The two PI's utilized the congress venue to discuss their joint research program between themselves and with other interested participants attending the congress The congress was also accompanied with an exhibition of state-of-the-art solar technologies, both commercially available and presently under development

F Future Work

The research program is progressing in accordance with the Time Chart as cited in the original research proposal During the meeting of the PI's in Taejon, Korea in August 1997, it was agreed that no major changes in the TECHNICAL WORK PLAN were necessary at this time The focus during the coming year will be in testing large systems consisting of a number of modules, analyzing the results, validating the mathematical model of the still and incorporating nocturnal heating in the solar still system The construction of the prototype hybrid solar still system utilizing a waste thermal energy source will be undertaken during the third year of the program

During the third year of the program the BGU group will begin testing a recently constructed third generation 2 m^2 solar still fabricated from stainless steel This still is similar in design to that of the second generation still which was fabricated from galvanized iron with some modifications These modifications were applied to the previous design as a result of the experience gained from the testing of its predecessor It is anticipated that the large solar still system to be constructed during this year will be based on this design The RLIC group plan to begin the construction and testing of an innovative variation of their original module constructed, in part, from polymeric materials The intention of this module, which is presently in the design stage, is to eliminate both the double tray required by the original still module and the use of non-corrosive materials of construction The design envisions a closely-spaced parallel array of glass tubes joined at the bottom of edge of the still into a single manifold This array is sits upon a wick placed upon the inner surface of the still bottom and covered by a second wick stretched across the top of the glass tubes The air stream (once again the air is drawn into the still by placing the pump after the exit from the still) flows between the glazing and the upper wick surface and is saturated and then turns around at the top of the still and condenses during its flow through the glass tube array on the tube walls, which are relatively cooler as a result of the wetted outer surface This results in the recycle of the thermal energy It is contemplated that the feedstock enter the still module at its bottom edge, transported via a black polymeric tube, inserted above the upper wick, and released at the top edge of the still The feedstock is thereby preheated by the solar radiation

V SECTION II

A Managerial Issues

The Financial Status Reports have been submitted by the RLIC to the BGU Department of Contracts as scheduled and the financing of the project via bank transfers from Israel to Hungarian has proceeded smoothly The expenditure of the budget item are prorated

The main items purchased during this past fiscal year were the following
a RLIC- two HP DeskJtet color printers and a conductivity meter for monitoring the quality of the still product
b BGU- a gas flow meter to measure the more accurately the flow rate of the air stream through the solar still and a conductivity meter for monitoring the quality of the still product

The RLIC research group's technician, Ms Sára Perlaky-Jozan, retired in October 1997 Mr Bela Mezo, an electrical engineer specializing in in process control, joined the research group on a part-time basis (52 hours per month) in November 1997

In the framework of the consolidation program for the research institutes of the Hungarian Academy of Sciences, the RLIC has had its name changed to Environmental and Materials Chemistry During November and December 1997 it will be in the process of moving to the newly established Hungarian Chemical Center as an independent laboratory

As reported in our first MANAGEMENT REPORT, submitted in April 1996, the delay in the practical starting date of this project will be reflected in its progress and will, in all likelihood, require a no cost extension past it's official culmination date of about three months, viz , until January 31, 1999

B Budget

There were no major changes in any budget items Their participation in the ISES '1997 Solar World Congress afforded the two PI's an ideal venue for discussing the project and the planned visit of the Hungarian PI to Israel has been postponed and tentatively scheduled for April 1998 The only changes are in the time schedule of execution, viz , the execution of some budget items have been delayed to the third year of the project, a result of the delay in initial starting date of the grant

C Special Concerns

Does not apply to this project

D Collaboration, Travel, Training and Publications

The close collaboration between the two PI's has and their respective research groups has escalated over the past year The collaborative efforts have been facilitated by a continuous dialogue via email and when necessary fax This was especially true with regard to the preparation of the two manuscripts submitted for the Proceedings of the International Solar Energy Society Conference, Solar World Congress 1997, Taejon, Korea, Aug 1997 A manuscript, entitled "Design parameters, performance testing and analysis of a double-glazed, air-blown solar still with thermal energy recycle", has been submitted to Solar Energy, the official journal of the International Solar Energy Society This describes in detail the most recent experimental results on the second generation solar still module A second manuscript reporting on the solution of the set of nonlinear

differential equations describing the solar still module system by numerical integration is presently under preparation

The Israeli PI, Dr A Kudish and the Hungarian PI, Dr G Mink, together with Mr L Horvath traveled to Korea in August and participated in the International Solar Energy Society's Solar world Congress Dr Mink presented a paper entitled "Design and performance of an air-blown, multiple-effect solar still with thermal energy recycle" and Dr Kudish presented a paper entitled "Heat transfer processes in an air-blown, multiple-effect solar still with thermal energy recycle" The discussions following the presentations have been incorporated into both the final versions of the manuscripts submitted for publication in the Congress Proceedings and into the new manuscripts mentioned above In addition, both PIs were honored by being chosen as session chairpersons at the meeting The meeting of PIs was utilized to plan the research program for the next six months, including some design variations on the solar still module

The scheduled travel plans for the third year of the research program have been tentatively set as follows

1 Dr Mink will travel to Israel during the second half of April 1998 to discuss the progress of the research program and set the goals for the remainder of study

2 Dr Kudish will travel to Hungary during the second half October 1998 to begin to plan to final phase of the program As mentioned in all our previous reports, we are requesting an extension of the terminal date of research program until January 31, 1999, since the actual funding of the grant did not start until February 1, 1996 In addition, there is a distinct possibility that the two PIs may take the opportunity of Dr Kudish's visit to Budapest to travel to Croatia for a Solar Energy conference scheduled for that time to present papers describing the results of their research program

A LIST OF PROJECT PUBLICATION REPRINTS

i G Mink, M M Aboabboud, L Horvath, E G Evseev and A I Kudish, Design and performance of an air-blown, multiple-effect solar still with thermal energy recycle *Proc Int'l Solar Energy Society Conference, Solar World Congress 1997,* **6,** 135-144, Taejon, Korea, Aug 1997

ii A I Kudish, E G Evseev, M M Aboabboud, L Horvath and G Mink, Heat transfer processes in an air-blown, multiple-effect solar still with thermal energy recycle *Proc Int'l Solar Energy Society Conference, Solar World Congress 1997,* **6,** 158-167, Taejon, Korea, Aug 1997

iii DESIGN PARAMETERS, PERFORMANCE TESTING AND ANALYSIS OF A DOUBLE-GLAZED, AIR-BLOWN SOLAR STILL WITH THERMAL ENERGY RECYCLE Submitted to *Solar Energy* (28 10 97)

E Request for USAID or BOSTID Actions

Does not apply at the present

APPENDIX

Proceedings International Solar Energy Society Conference, Solar World Congress 1997, 6, 135-144, Taejon, Korea, August 1997

DESIGN AND PERFORMANCE OF AN AIR-BLOWN, MULTIPLE-EFFECT SOLAR STILL WITH THERMAL ENERGY RECYCLE

G MINK , M M ABOABBOUD*, L HORVATH , E G EVSEEV * and A I KUDISH**
Research Laboratory for Inorganic Chemistry, Hungarian Academy of Sciences, 1518 Budapest Pf 132, HUNGARY, Tel +36 1 3193119, Fax +36 1 3192537, E-mail mink@sparc core hu
**Solar Energy Laboratory, Department of Chemical Engineering, Ben-Gurion University of the Negev, Beer Sheva 84105, ISRAEL , Tel +972 7 6461488, Fax +972 7 6472916, E/mail akudish@bgumail bgu ac il

Abstract - An air-blown, multiple-effect solar still with thermal energy recycle consisting of an upper evaporation chamber and lower condensation chamber, the prototype originally proposed by the scientist at the Research Laboratory for Inorganic Chemistry (Mink et al 1988), is being developed and tested under a joint Israeli-Hungarian research program The principle of operation of such a still, the main design parameters and the results of solar still performance tests will be presented The experimental procedures at both institutions are very similar, except that the Hungarian group utilizes a solar simulator and the Israeli group natural solar radiation (i e , out-door testing) to measure the solar still performance The present discussion will be restricted to the performance testing of a solar still with a nominal still area of 1 m^2 (1 86 m x 0 54 m) utilizing a solar simulator providing a constant radiation intensity of approximately 650 W m^{-2} The solar still performance was tested as a function of both feedstock and air flow rates The former was varied in the range between 2 28 to 4 09 kg h^{-1} and the latter between 1 9 and 9 4 kg h^{-1} It was observed, under these conditions, that the thermal energy recycle began to be effective after about 30 minutes and that the still achieved steady-state after approximately one hour of operation The solar still performance exhibits only a slight dependence on the feedstock flow rate, as predicted by theoretical considerations On the other hand, the steady-state distillation rate exhibits an optimum (of the order of 1 kg m^{-2} h^{-1}) as a function of increasing air flow rate The experimental results indicate that the still performance can be enhanced further by decreasing both the air flow rate and the cross sectional flow area in the lower condensation chamber

1 INTRODUCTION

The rationale behind the design of this air-blown, multiple-effect solar still was to overcome the inherent disadvantage in the operation of single-effect solar stills, viz , their efficiency, notwithstanding intensive research and development efforts, remains stalled in the 30-40% range (Delyannis and Delyannis (1980), Malik et al (1982) and Kudish (1991)) This air-blown, multiple-effect solar still is designed to recycle the thermal energy (i e , the latent heat of condensation), which is dumped/vented to the ambient in single-effect solar stills, to heat or pre-heat the feedstock to the solar still

The mode of operation of the solar still will be described together with experimental results in the following sections A companion paper presented separately (Kudish et al (1997)) describes two mathematical models for the heat transfer processes ocurring in this solar still system

2 SOLAR STILL DESCRIPTION

A schematic diagram of the air-blown, multiple-effect solar still is presented in Fig 1 It is essentially of the tilted-wick genre in the form of a thin rectangular box divided into two chambers (upper evaporator and lower condenser) by a central metal sheet There is a slot between the two chambers at the top of the tilted still (viz , the central metal sheet does not extend across the full length of the still but leaves a slot of 10 mm between its top end and the still's upper extremity) The metal sheet also functions as (i) the support for the wick (a black porous material) which covers it on the upper chamber side, (ii) the surface to which a serpentine tube, on the lower chamber side, for transporting the feedstock to the upper chamber, is attached This serpentine tube also functions as a heat exchanger for pre-heating the feedstock prior to entering the upper chamber The spacing between the central metal plate and the upper chamber still glazing and the lower chamber backside are both < 15 mm

The mode of operation of the solar still is as follows (1) ambient air is pumped into the upper chamber from the bottom of the tilted still and sweeps the water vapor evaporated from the tilted wick into the lower chamber via the slot at the top of the tilted still (maximum temperature of the air stream is measured at this point, above the slot, prior to entering to the lower chamber and serving as the hot fluid in what is essentially an air-liquid heat exchanger), (2) the major portion of the water vapor then condenses on the backside of the metal sheet supporting the wick or on the serpentine tube, which enters at the bottom of the lower chamber, transporting the

feedstock to the upper chamber, (3) the feedstock, which enters the serpentine tube at a flow rate in excess of the rate of evaporation from the wick in the upper chamber and is preheated during its passage through the serpentine tube, exits the serpentine tube at the top edge of the central plate and passes over a weir and flows by gravity down the wick, (4) the distillate exits the lower chamber and is collected, whereas the saturated air stream, also exiting the lower chamber, enters an external condenser, to further condense the water vapor remaining prior to venting to the ambient

In the upper chamber the air stream flows countercurrently to the direction of feedstock flowing down the wick, whereas in the lower chamber the air stream flows both countercurrently and perpendicular to the direction of the feedstock flowing through the serpentine tube Due to the nature of this solar still, viz , that the upper chamber glazing does not serve as a condensation surface, it is possible and recommended to utilize a double glazing to reduce thermal energy losses via the glazing to the ambient In fact, it is possible to use non-wetting polymeric glazings such as those used as transparent insulating material (TIM's), e g , Qualex, a double-walled polycarbonate sheet, as the solar still glazing

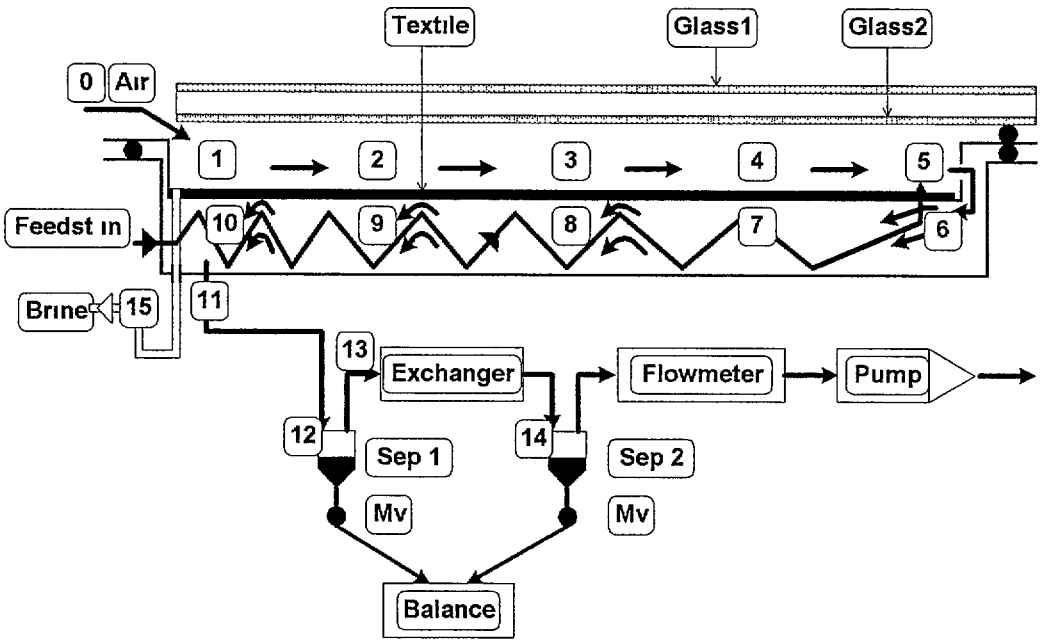

Fig 1 Schematic diagram of the air-blown, multiple-effect solar still, where 0 -15 denote thermistors and Mv, magnetic valves

3 MEASUREMENTS

Experimental setup

The experimental setup (cf Fig 1) consists of the following solar still module solar simulator (not shown) two vapor/liquid separators for collecting the product, heat exchanger, peristaltic pump to transport the feedstock, low pressure adjustable flow rate air pump, electric balance to measure distillate, gas flow meter magnetic valves to drain periodically the separators, electric balance to measure the amount of the drained distillate and temperature sensors The system is connected on-line to a personal computer for data collection and analysis The position of the air pump ensures that the system operates at a pressure somewhat below ambient

Solar still module

The still consists of two shallow trays, supplied with perimeter rims, of slightly different dimension (see below) such that the upper tray can be inserted into the lower tray Air tightness was ensured by inserting a rubber gasket tape between the rims and between the upper rim and glazing The two trays and glazing were clamped together by screws The upper and lower trays were constructed from a 1 mm thick copper sheet and the lower tray was insulated externally (i e , its bottom and perimeter) with 50 mm thick polyurethane foam The two tray design separates the solar still into two chambers connected by the slot in the upper chamber The brine drain-off tube is soldered to the bottom of the upper tray (viz , in tilted position) and passes through the lower tray

The evaporation plate, i e , the upper tray is covered by a thin black porous fabric (wick) The serpentine tube carrying the feedstock in the lower chamber is attached to the bottom of the upper tray and the feedstock exits the serpentine tube onto the upper tray via its slot (cf Fig 2) and is evenly distributed over the width of the wick by means of an overflow weir near the top of the upper tray The solar still module dimensions are as follows

Double-glazing	3 mm thick glass, L = 1 95 m, W = 0 6 m, spacing between glazing = 20 mm
Upper chamber	1 mm thick copper, L = 1 87 m, W = 0 545 m, H = 12 mm, rim width = 30 mm on three sides and 40 mm at top (adjacent to slot) Spacing between the two chambers = 12 mm
Wick	0 3 mm thick black porous fabric, L = 1 85 m, W = 0 545 m, A = 1 m^2, weir height = 6 mm, Spacing between textile and inner glazing = 12 mm It is assumed that the wick thickness is independent of water load
Lower chamber	1 mm thick copper, L = 1 9 m, W = 0 55 m, H = 25 mm, rim width = 30 mm
Serpentine tube	copper, L = 6 m, D_I = 10 mm, D_O = 12 mm, A = 0 20 m^2
Baffles	nine baffles soldered to the bottom of lower chamber, H = 12 mm for all baffles, seven, L = 0 44 m, one, L = 0 36 m, one, L = 0 28 m
Still casing	wood, L = 2 06 m, W = 0 7 m, H = 90 mm, bottom thickness = 10 mm, side thickness = 15 mm
Bottom and edge insulation	50 mm thick polyurethane foam, conductivity = 0 04 W m^{1} K^{1}

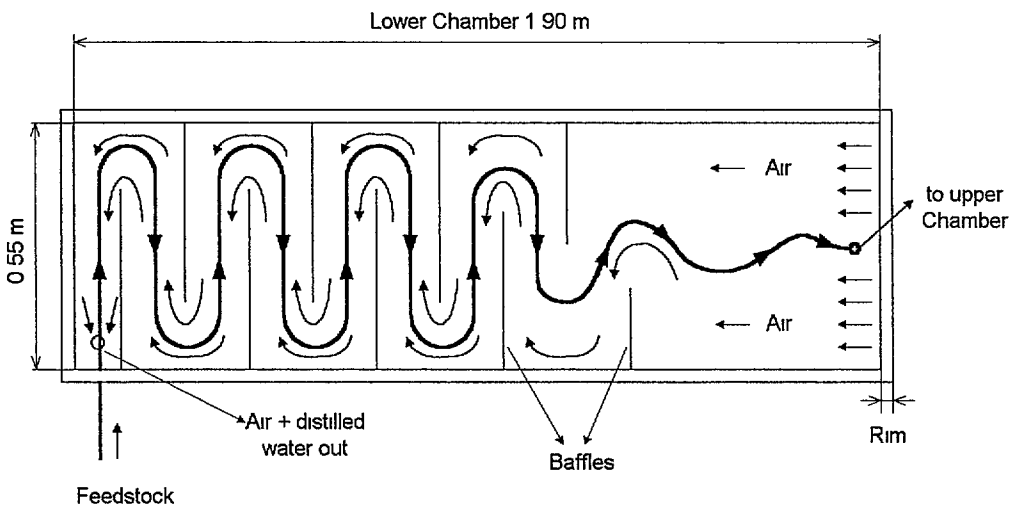

Fig 2 Top view of the lower chamber with serpentine tube and baffles (not drawn to scale)

Experimental conditions and procedure

The tilt angle of the solar still module was set at 20° throughout this study Similarly, the solar radiation intensity provided by the solar simulator was 650 +/-10 W m^{2} and its tilt angle was also 20° The differential and cumulative yields from Separator I and II were measured automatically by a type PT 6 Satorius electric balance with an accuracy of ± 1 g The temperatures were measured with an accuracy of ± 1 °C using calibrated temperature sensors of the silicon base type KTY 11-2A The absolute humidity of air in the vicinity of the slot was calculated from the material and energy balances on the still A data acquisition system served to monitor and store the temperature data from the sixteen thermistors and to calculate differential and cumulative yields at variable time intervals It consisted of a PC with an A/D-D/A converter card, electronic measuring and magnetic valve control unit, temperature sensors and a digital balance with a RS232C serial interface The data acquisition, control and analysis software were developed for the study

The experimental procedure for the performance testing is as follows

(1) the air and feedstock flow rates are defined and held constant,

(2) the temperatures at a number of strategically placed locations are monitored

air stream- upper chamber inlet, equally spaced probes in the direction of flow and above the slot,
lower chamber below the slot, equally spaced probes in the direction of flow and at the outlet,
feedstock- lower chamber inlet,
upper chamber overflow weir and brine drain-off outlet,
saturated air stream exiting the still to the external condenser,

(3) the distillation rate is determined by measuring the cumulative distillate during a specified time interval

4 RESULTS

The results refer to the performance testing of a solar still with a nominal still area of 1 m^2 (1 86 m x 0 54 m) utilizing a solar simulator providing a constant radiation intensity of approx 650 W m^{-2} The solar still performance was tested as a function of both feedstock and air flow rates The former was varied in the range between 2 28 to 4 09 kg h^{-1} and the latter between 1 9 and 9 4 kg h^{-1} The solar still achieved steady-state as evidenced by monitoring both air stream temperatures and the distillation rate, after approximately one hour of operation The maximum air stream temperature, ~ 80°C, is measured at the top of the upper chamber above the slot It is observed that thermal energy recycle begins to take effect after about 30 minutes by comparing the continuously monitored air stream temperatures at the inlet to the upper chamber to that at the outlet from the lower chamber, viz , after about 30 minutes the latter exceeds the former The steady-state distillation rate was found to be of the order of 1 kg m^{-2} h^{-1} It is of interest to note, that if the air pump remained in operation after the solar simulator was shut-off and the system was at steady-state, the still continued to produce distillate, albeit at a decreasing rate, for about another hour In other words, in spite of the relatively low thermal mass of the solar still module, thermal energy recycling is still capable of enhancing the yield after 'sunset', i e , after the solar simulator is shut-off

Productivity as a function of air and feedstock flow rates

During the course of performance testing it was observed that the solar still module, under steady-state conditions, was capable of producing distillate at a rate of 1 kg m^{-2} h^{-1} over a relatively wide range of both air and feedstock flow rates The air flow rates could be varied in the range of 1 9 to 3 6 kg m^{-2} h^{-1} and the feedstock flow rate between 2 to 4 kg m^{-2} h^{-1} without seriously affecting the overall productivity rate

The productivity rates for two different feedstock flow rates, 2 28 and 4 07 kg m^{-2} h^{-1} and air flow rates in the range of 1 9 to 9 4 kg m^{-2} h^{-1} are presented in Table 1 Also listed in Table 1 is the temperature of the air stream that enters the lower chamber, T_{l1} It is observed that both T_{l1} and DI the rate of condensation in the lower chamber, decrease monotonically with increasing air flow rates On the other hand,, DII, the rate of condensation in the external condenser, exhibits a moderate increase with increasing air flow rates Consequently, a monotonic decrease of the total productivity rate ΣD is observed, It obvious that an optimum flow rate must exist since for this solar still design the productivity is zero for a zero air flow rate

Table 1 Dependence of distillation rate as collected in Separator I (DI) and Separator II (DII) and the temperature of the wet air entering the lower chamber T_{l1} on the air flow rate and feedstock flow rate for a still area = 1m^2 and radiation intensity = 650 W m^{-2}

Feedstock flow rate = 2 28 kg h^{-1}					Feedstock flow rate 4 07 kg h^{-1}				
m_a kg h^{-1}	DI kg h^{-1}	DII kg h^{-1}	Σ D kg h^{-1}	T_{l1} °C	m_a kg h^{-1}	DI kg h^{-1}	DII kg h^{-1}	Σ D kg h^{-1}	T_{l1} °C
1 95	0 796	0 202	0 998	85 1	1 85	0 786	0 184	0 970	84 5
3 51 3 61	0 696 0 674	0 294 0 287	0 990 0 971	76 8 76 2	3 25	0 682	0 214	0 896	75 4
4 96	0 539	0 305	0 844	69 2	4 84	0 580	0 256	0 836	68 2
6 46	0 462	0 315	0 777	64 7	6 48	0 496	0 288	0 784	62 7
7 37	0 424	0 316	0 740	61 8	7 29	0 455	0 308	0 763	60 1
9 40	0 371	0 321	0 692	59 2	8 55	0 390	0 286	0 676	57 0

It is also apparent from Table 1 that in the range studied, the effect of feedstock flow rate on the solar still productivity is negligible However, in the vicinity of the optimum air flow rate a lower feedstock flow rate results in slightly enhanced productivity This suggests that the still be operated at that lowest feedstock flow rate capable of maintaining the wick completely wet, viz , a 2 kg m^2 h^{-1} feedstock flow rate

Thermal characteristics of the still at about optimum feedstosk flow rate

The sensitivity of a number of still parameters to changes in the rate of air flow is shown in Table 2 These include the still maximum temperature T_{l1}, the dew point of the air stream entering the lower chamber T_{Dew}, the temperature of the saturated air exiting the lower chamber T_{lo}, the thermal energy recycled directly to the wet wick surface q_R, the thermal energy utilized to preheat the feedstock q_{PR}, the total thermal energy recycled q_{RT} the utilized solar energy Q_U and the top thermal energy losses from the still q_{wa} The thermal energy parameters were determined from the mass and energy balances on the still at a fixed feedstock flow rate m_f = 2 28 kg m^{-2}

Table 2 Variation in the solar still module maximum temperature T_{l1}, the dew point of the fluid entering the lower chamber T_{Dew}, the temperature of the fluid exiting the lower chamber $T_{l,o}$, the thermal energy recycled directly to the wet wick surface q_R, the thermal energy utilized to preheat the feedstock q_{PR}, the total thermal recycled q_{RT}, the utilized solar energy Q_U and the thermal energy losses to the ambient through the glazing q_{wa}, as determined from mass and energy balances on the solar still, as a function of air flow rate
Still area = 1 m^2, radiation intensity = 650 W m^{-2}, feedstock flow rate = 2 28 kg m^{-2} h^{-1}

m_a kg h^{-1}	T_{l1} °C	T_{Dew} °C	T_{lo} °C	q_R W m^{-2}	q_{PR} W m^{-2}	q_{RT} W m^{-2}	Q_U W m^{-2}	q_{wa} W m^{-2}
1 95	85 1	80 7	62 0	313	155	468	331	211
3 51	76 8	72 6	59 1	273	132	405	408	140
3 61	76 2	72 0	59 2	277	131	407	397	154
4 96	69 2	66 0	54 2	237	112	350	406	146
6 46	64 7	61 2	51 4	208	99	307	420	134
7 37	61 8	58 4	50 0	182	91	273	451	103

It is observed that with increasing the air flow rate, m_a varies in the range of 1 95 to 7 37 kg m^{-2} h^{-1}, the amount of total thermal energy recycled q_{RT} decreases by about 200 W m^{-2} At the same time the amount of utilized solar energy Q_u increases (the top thermal energy losses q_{wa} decrease) but this is only of the order of 100 W m^{-2} and consequently overall still performance is inferior It is suggested, based upon the experimental results reported in Tables 1 and 2, that the real operational optimum for the still should be at even lower air flow rates, viz , below 1 95 kg m^{-2} h^{-1}, provided that the module is designed such that the air velocity in the upper chamber is higher than 0 05 m s^{-1} (this is estimated as the minimum velocity necessary to hinder the back-diffusion of the vapors in the upper chamber) and, at the same time, turbulent flow is achieved in the lower chamber to ensure high heat transfer numbers

5 DISCUSSION

A discussion regarding the heat transfer processes occurring within the solar still module system is facilitated by referring to the schematic diagram in Fig 3 The values for the parameters, normalized to a solar still area of 1 m^2, used in this analysis were as follows

- G_a = solar radiation absorbed by the still components = 550 W m^{-2},
- q_{wa} = thermal energy loss from black wick to ambient = 200 W m^{-2},
- Q_u = solar energy utilized in the upper chamber = 350 W m^{-2},
- q_B = back and edge thermal energy losses through the solar still insulation to the ambient = 30 W m^{-2},
- q_R = thermal energy recycled from the lower cavity to the central plate = 350 W m^{-2}
- q_{PR} = thermal energy utilized in the lower chamber to preheat the feedstock = 130 W m^{-2},
- m_a = mass flow of air = 2 37 kg m^{-2} h^{-1} (equivalent to 2 m^3 m^{-2} h^{-1} dry air at 298 K and 101 3 kPa),
- m_f = feedstock flow rate in the serpentine tube = 2 2 kg m^{-2} h^{-1},
- m_{bo} = brine drain-off flow rate = 1 1 kg m^{-2} h^{-1},
- m_{co} = condensate (viz , distillate) flow rate at the outlet = 0 7 kg m^{-2} h^{-1}

The temperatures were assumed to be as follows $T_a = T_{u,i} = T_{f,i} \approx 30°C$, $T_{b\,o} \approx 60$ °C and $T_{l\,o} \approx T_{c\,o} \approx 65°C$ where subscripts a, u, f, b, l and c refer to ambient, air stream in the upper chamber, feedstock, brine air stream in the lower chamber and condensate, respectively Subscripts i and o denote in and out, respectively

As shown in Fig 3, in the upper chamber the enthalpy of the air stream is increased by the recycled thermal energy, q_R, the utilized solar energy Q_u and the thermal energy released by the preheated feedstock The maximum air stream enthalpy, within the solar still module, occurs at the slot connecting the two chambers In the lower chamber there is a marginal thermal energy loss through the edge and bottom insulation, q_B A considerable fraction of the thermal energy of the air stream in the lower chamber is recycled, both to preheat the feedstock and heat the evaporation plate, viz , the metal plate separating the two chambers Most of the vapor content of the air stream flowing through the lower chamber condenses on either the serpentine tube or the evaporation/metal plate The remaining thermal energy input to the solar still exits the unit as sensible heat of the condensate and the enthalpy of the saturated air stream

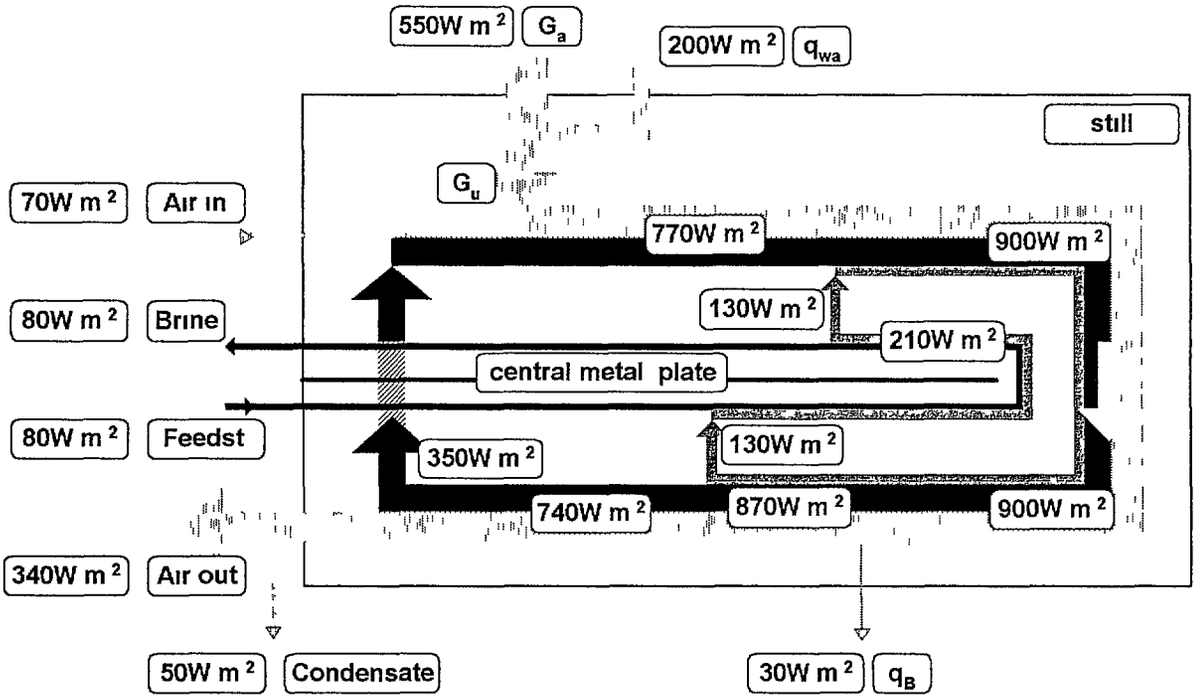

Fig 3 Estimated thermal energy flow diagram in air-blown, multiple-effect solar still with internal thermal energy recycle, normalized to a unit still area See text for nomenclature assumed flow rates and temperature values

System design parameters

i Feedstock and air flow rates- Previous investigations by Mink et al (1997) have shown that a feedstock flow rate $m_f = 2$ kg $h^{-1} m^{-2}$ is sufficient to completely wet the wick This study utilized a solar still with a still area, A, of 1 m^2 tilted at an angle of 20° The radiation intensity was 650 W m^{-2}, utilizing a solar simulator and the evaporation rate m_e was approximately 1 1 kg h^{-1} It was also observed that the highest productivity was obtained for air flow rates m_a in the range between 1 8 and 3 5 kg m^{-2} h^{-1} Consequently, in the present study the feedstock flow rates m_f, were in the range of 2 28 to 4 07 kg m^{-2} h^{-1} and the air flow rates were varied between 1 9 and 9 4 kg m^{-2} h^{-1}

ii Utilization of the vapor content of the air stream exiting the solar still- The condensation in the lower chamber was estimated in the above example, cf Fig 3, as 0 7 kg m^{-2} h^{-1} Based upon this calculation, the saturated air stream exiting the lower chamber is also a potential source of fresh water If Q_{lo} denotes the enthalpy of the saturated air in J kg^{-1} for the case when 1 kg air is saturated at a given temperature T the rate of thermal energy exiting with air stream q_{lo} is given by

$$q_{lo} = m_a Q_{lo} \qquad (1)$$

It is observed from Fig 3, that for a still area of 1 m^2 and m_a = 2 37 kg $m^{-2} h^{-1}$, that q_{lo} = 340 W m^{-2} and Q_{lo} = 516 500 J kg^{-1} This value corresponds to a $T_{lo} \approx 65°C$ and an absolute humidity H_{abs} of about 0 20 kg vapor per kg air, as determined from Psychrometric Tables The mass flow rate of vapor that exits within the air stream from the unit is ≈ 0 48 kg h^{-1} (i e , as determined from A $m_a H_{abs}$) Provided that the temperature of the exiting air stream can be cooled, by an external heat exchanger (viz , a condenser), such as to approach the ambient temperature, an additional 0 4 kg $m^{-2} h^{-1}$ fresh water can be recovered

On the other hand, $m_a Q_{lo}$ is also equivalent, as determined from an overall thermal energy balance on the solar still, to

$$m_a Q_{lo} = Q_u + m_a Q_{u,i} + c_w m_f T_{f,i} - c_w m_{bo} T_{bo} - c_w m_{co} T_{co} - q_B \quad (2)$$

where c_w is the heat capacity of water in J °C^{-1} kg^{-1} If it is assumed that the temperatures are as cited above viz , $T_a = T_{u,i} = T_{f,i} \approx 30°C$ and $T_{bo} \approx 60°C$ and the still operates near the optimum, than the evaporation rate is about half the feedstock flow rate Consequently, the sum of the 3rd and 4th terms in Eq 3 approach zero since the brine drain-off rate is about half of that of the feedstock In addition, for relatively low air flow rates i e , near optimum operating conditions, the thermal energy input from the entering air stream $m_a Q_{u,i}$ is low (≈ 50 - 100 W m^2), similarly for the thermal energy exiting the still via the condensate (≈ 50 W m^2 for m_{co} = 0 7 kg $m^{-2} h^{-1}$ and $T_{co} \approx 65°C$) Finally, q_B, the back and edge thermal energy losses through the solar still insulation to the ambient can be reduced to ≈ 30 W m^{-2} by standard and inexpensive insulation materials As a result of the above, the sum of the 2nd, 5th and 6th terms also approach zero and Eq 2 reduces to

$$m_a Q_{lo} \approx Q_u \quad (3)$$

and

$$Q_{lo} \approx Q_u m_a^{-1} \quad (4)$$

It is apparent from the above analysis that the enthalpy of the saturated air stream exiting the lower chamber is approximately equivalent to the utilized solar energy Q_u, and is inversely proportional to the air stream flow rate m_a Consequently, it would be advantageous to operate the solar still at even lower air stream flow rates since higher exiting air stream enthalpy values translate into both higher temperatures and vapor content of the exiting air stream Also, the overall heat transfer coefficient for condensation from the air stream decreases rapidly with decreasing temperature (see below) The lower air stream flow rates will result in an increase in the air stream temperature in both chambers and an increase in the external condenser efficiency i e as a result of the greater temperature gradient An increased condenser efficiency will allow a reduction in condenser size and/or cooling energy requirement and resultant decrease in construction and/or operating costs
As mentioned previously, an optimum air stream flow rate must exist in the range of relatively low flow rates, since for this solar still design the productivity will be zero for an air flow rate of zero

iii Vapor/liquid separator, heat exchanger- In the performance testing of the solar still module in the laboratory it was desired to measure the primary distillation/productivity rate within the module (i e , the rate of condensation within the lower chamber, which is a direct measure of the efficiency of the thermal energy recycle process) and that obtained from the exiting air stream, secondary distillation Therefore, the vapor/liquid mixture exiting the still module first entered vapor/liquid Separator I (primary distillate), then the vapor stream was passed through a heat exchanger/condenser prior to entering vapor/liquid Separator II (secondary distillate) In a scaled-up system it would be sufficient to have the outlet vapor/liquid mixture exiting the system to pass through a heat exchanger/condenser prior to entering a single vapor/liquid separator

In the present study a simple water cooled condenser functioned as the heat exchanger but it would be very advantageous to utilize the non-negligible thermal energy present in this stream to preheat the feedstock viz , to utilize the feedstock as the cooling medium In such a design the temperature of feedstock entering the still would approach T_{lo} and thereby further increase the still operating temperatures This method of operation of the solar still is discussed in detail by Aboabboud et al (1996)

iv Glazing- The amount of solar radiation absorbed within the still G_a is the difference between the incident solar radiation G and the reflection losses from the still glazing G_r, cf Fig 3 The utilized solar energy

Q_u is determined from the difference between the G_a and the thermal energy losses to the ambient through the glazing q_{wa} Thus, the amount of utilized solar energy is given by

$$Q_u = G - G_r - q_{wa} \quad (5)$$

It is apparent from Fig 3, that for a given solar irradiance G, the still performance is determined mainly by the top losses q_{wa} and the efficiency of the thermal energy recycle processes Since the system is designed to operate at low mass flow rates of air and at relatively high temperatures, the thermal energy losses to the ambient will increase with increasing temperature To minimize these thermal energy losses the glazing should have good insulating properties This was achieved by utilizing a double glazing The disadvantage of a double glazing is the increased reflection losses, approximately an 8 % increase in reflection losses, but this is more than compensated for by the relatively higher temperature gradients, $\Delta T = T_w - T_a$, achieved In addition since the glazing does not function as a condensation surface (in fact, if condensation is observed on the glazing the system is not operating properly) it is possible to use such polymeric glazings defined as transparent insulating materials (TIM s), e g Qualex, a transparent double-walled polycarbonate sheet, which are, in general, non-wetting

v Thermal energy recycle process and air velocity in the lower chamber- The thermal energy recycle process occurs in the lower chamber via heat transfer from the saturated air stream to the central metal plate and to the serpentine tube The rate of condensation in the lower chamber (ca 0 7 kg m^{2} h^{1}) is directly related to these processes The heat transfer processes include condensation and convective heat transfer from the air stream The combined heat transfer coefficient h_{cg}, which strongly depends on the temperature (the vapor content of saturated air) and its fluid mechanical properties is approximated by

$$h_{cg} = 1/ [(1/ h_c) + q_g/(q\ h_g)] \quad (6)$$

where h_c is the heat transfer coefficient for the condensed water film, in the range of 5000 - 10000 W m^{2} K^{1}, h_g is the convective heat transfer coefficient of the gas film, q_g is the heat transmitted by gas (air + non-condensing vapor) and q is the total heat transmitted

The overall heat transfer coefficient U_{lw} for thermal energy recycle process from the lower chamber to the upper surface of the wet wick, where the evaporation process is occurring, is given by

$$U_{lw} = 1/ [(1/ h_{cg}) + (1/ h_m) + (1/ h_{sd}) + (1/ h_f) + (1/ h_w)] \quad (7)$$

where h_m is the heat transfer coefficient for the metal plate, 260 000 W m^{2} K^{1} for a 1 mm thick copper sheet, h_{sd} is the heat transfer coefficient for scale deposit , approximately 5000 W m^{2} K^{1}, h_f is the heat transfer coefficient for the brine film above the plate, about 3500 W m^{2} K^{1} and h_w is the heat transfer coefficient for the wet wick, about 660 W m^{2} K^{1} for a 1 mm thick water film

The above equations for the heat transfer coefficients were solved by determining values for q_g/q from the Psychrometric Tables for temperature intervals of 5 °C and using the above values for the individual heat transfer coefficients The following values for the heat transfer coefficient for the gas film h_g were considered 80, 20, 10 and 5 W m^{2} K^{1} The results of this analysis are reported in Table 3 A value of h_g = 80 W m^{2} K^{1} corresponds to turbulent flow with Re > 10 000 and a gas velocity of 10 m s^{1} or above for the case of an equivalent diameter D_e of approximately 0 02 m Using the same value for the equivalent diameter, h_g values of 20, 10 and 5 W m^{2} K^{1} correspond to approximately 2, 1 and 0 5 m s^{1} gas velocities, respectively

It is obvious from the results of this analysis reported in Table 3 that the effectiveness of thermal energy recycle process and consequently the still performance depends mainly on U_{lw} It is possible to increase, to a limited extent, the value of U_{tw} by decreasing the thickness of the porous wick, cf Table 3

The results reported in Table 3 suggest that the still should be operated at high temperatures and with high gas film heat transfer coefficient h_g values Such high temperatures can be achieved only if sufficiently low mass flow rates are applied, since at constant energy input the enthalpy gain of the air stream is inversely proportional to its mass flow rate On the other hand, high linear air stream velocities are necessary in the lower chamber in order to achieve high heat transfer coefficient h_g This goal can be achieved by decreasing the height of the lower chamber and/or by accelerating the air stream velocity with the help of baffles, since the air mass flow must be low

Table 3 Overall heat transfer coefficient for thermal energy recycle U_{lw} as a function of temperature and the heat transfer coefficient for the gas film h_g for a wick thickness of 1 mm

T, °C	90	85	80	75	70	65	60	55	50	45	40	35
$h_g = 80\ W m^{-2} K^{-1}$ U_{lw}, W m^{-2} K^{-1}	437	425	413	398	382	362	343	320	297	273	246	223
$h_g = 20\ W m^{-2} K^{-1}$ U_{lw}, W m^{-2} K^{-1}	391 436*	358 393*	324 354*	290 315*	258 277*	225 240*	198 209*	169 177*	146 152*	124 128*	104 107*	88 90*
$h_g = 10\ W m^{-2} K^{-1}$ U_{lw}, W m^{-2} K^{-1}	342	292	251	213	180	150	126	104	87	72	59	49
$h_g = 5\ W m^{-2} K^{-1}$ U_{lw}, W m^{-2} K^{-1}	275	215	173	139	113	90	73	59	48	39	31	26

* for wick thickness = 0 5 mm

In the present solar still module the feedstock is preheated in the lower chamber and its height is determined by the outer diameter of the serpentine tube Therefore, in the lower chamber the gas velocity was accelerated, by a factor of about three by means of baffles, which were concentrated in the lower temperature/section of the chamber (cf Fig 2)

vi Serpentine tube area vs still area- The ratio of the thermal energy transmitted to the serpentine tube to that directly recycled to the central plate is 130/350 ≈ 0 37, cf Fig 3 Ideally, the ratio of the tube to plate surface area should be identical to the thermal energy recycle ratio, since the nature of heat transfer process to the tube and the plate is essentially the same Nevertheless, if it is assumed that the average temperature gradient between the tube and plate is $T_{p\,av} - T_{t,av} \approx 2$ K, and considering that the overall heat transfer coefficient U_{lw} is in the range between 200 - 300 W m^{-2} K^{-1} i e , the still operates under nearly optimum condition, it is possible to reduce the tube to plate surface area ratio to about 0 2 m^2 m^{-2}, in order to achieve cost savings This would be more than sufficient if the entering feedstock is preheated close to T_{1o} utilizing the enthalpy present in the air stream exiting the solar still

vii Pressure drop in the system- A drawback in increasing the air stream velocity in the lower chamber is that parasitic electric energy required to drive the air pump also increases This may be a major problem in rural application where the electric energy may be supplied by PV panels In addition, a system operating under high pressure drops requires sturdier and more expensive construction than that operating at nearly atmospheric pressure The present solar still system was designed for very low (< 100 Pa) pressure drops and may be considered to operate under atmospheric conditions

6 CONCLUSIONS

The design and performance testing of a double glazed, air-blown, multiple-effect solar still with thermal energy recycle consisting of two chambers, upper evaporator and lower condenser, has been presented A considerable fraction of the latent heat of condensation is recycled for directly heating the evaporation plate and for preheating the feedstock and thereby enhancing the rate of the evaporation process

The heat transfer processes are based upon film condensation from a saturated air stream, which is characterized by a relatively high heat transfer coefficient, especially when operating at relatively high temperatures These high temperatures are achieved by operating the solar still system at low air mass flow rates In addition, the heat transfer process is further enhanced by the high air velocities in the lower (condensation) chamber

The solar still performance, as expected from theoretical analysis depends only slightly on the feedstock flow rate and the steady-state distillation rate exhibits an optimum (that was found to be of the order of 1 kg m^{-2} h^{-1}) with increasing air flow rates

The experimental results suggest that the solar still performance can be further enhanced by decreasing both the air flow rate and the cross sectional flow area in the lower chamber

Acknowledgment- This research was supported under Grant No TA-MOU-95-C15-050, US-Israel Cooperative Development Research Program, Office of Agriculture & Food Security, Center for Economic Growth, Bureau for Global Programs, Field Support and Research, USAID

REFERENCES

Aboabboud, M M , Horvath, L , Szepvolgyi, J , Mink, G , Radhica E and Kudish, A I (1996) The use of a thermal energy recycle unit in conjunction wit a basin-type solar still for enhanced productivity *Energy* **23**, 83-91

Delyannis, A and Delyannis, E E (1980) *Seawater and Desalting*, Vol 1 pp 67-70 Springer-Verlag, Berlin

Kudish, A I (1991) Water Desalination In *Solar Energy in Agriculture-Energy in World Agriculture* Parker B F (Ed), Vol 4, pp 255-294 Elsevier Science Publishers B V , Amsterdam

Kudish, A I , Evseev, E G , Aboabboud, A A , Horvath, L and Mink, G (1997) Heat transfer processes in an air-blown, multiple-effect solar still with thermal energy recycle, submitted to "Solar Means Business" 1997 ISES Solar World Congress, Korea

Malik, M A S , Tiwari G N , Kumar, A and Sodha, M S (1982) *Solar Distillation* Pergamon Press, Oxford

Mink, G Jakabos, D and Szekely, T (1988) Hungarian Patent, 201,714

Mink, G Aboabboud, M M and Karmazsin, E (1997) Air-Blown Solar Still with Heat Recycling, *Solar Energy* (in press)

Proceedings International Solar Energy Society Conference, Solar World Congress 1997, 6, 158-167, Taejon, Korea, August 1997

HEAT TRANSFER PROCESSES IN AN AIR-BLOWN, MULTIPLE-EFFECT SOLAR STILL WITH THERMAL ENERGY RECYCLE

A I KUDISH, E G EVSEEV*, M M ABOABBOUD *, L HORVATH * and G MINK *
Solar Energy Laboratory, Department of Chemical Engineering, Ben-Gurion University of the Negev, Beer Sheva 84105, ISRAEL, Tel +972 7 6461488, Fax +972 7 6472916, E/mail akudish@bgumail bgu ac il
Research Laboratory for Inorganic Chemistry Hungarian Academy of Sciences 1518 Budapest Pf 132, HUNGARY, Tel +36 1 3193119, Fax +36 1 3192537, E-mail mink@sparc core hu

Abstract - Mathematical models have been developed independently by the scientists at the two institutions involved in a joint research program to describe the heat and mass transfer processes occurring in an air-blown, multiple-effect solar still with thermal energy recycle The solar still is of the tilted wick genre in the form of a thin rectangular box divided into two chambers by a central metal sheet A slot between the two chambers at the top of the tilted still allows for passage of the air stream from the upper to the lower chamber The upper chamber functions as a an evaporator and the lower as a condenser The air stream sweeps the water vapor evaporated from the tilted wick via the slot into the lower chamber where it condenses and delivers the second-effect Both models utilize non-linear differential equations to describe the system under both transient and steady-state conditions The two groups differ in their approach to the solution of the non-linear differential equations The models predict air and water stream temperatures, water vapor content and the distillation rate The models were validated by a detailed comparative analysis of their predictive ability utilizing experimental measurements on such an air-blown, multiple-effect solar still with thermal energy recycle

1 INTRODUCTION

An extensive review of the literature on single-effect solar stills reveals, that in spite of the large amount of research and development effort invested in such stills, their efficiency remains stalled in the 30-40% range, i e, only this fraction of the incident solar radiation is utilized in the production of distillate (Delyannis and Delyannis (1980), Malik et al (1982) and Kudish (1991)) If we apply this finding to arid zones, which are characterized by the greatest shortages of potable water, one arrives at the following conclusion present day state-of-the-art single-effect solar stills cannot be expected to exceed an annual productivity limit of $1 m^3 m^{-2}$ This assumes that the cumulative annual global radiation incident on the Earth's surface in these arid regions is about 8×10^6 kJ $m^{-2} y^{-1}$ and the annual still efficiency is of the order of 30% The major drawback in the design of such single-effect solar stills is the dumping, in excess of 90%, of the solar energy converted to thermal energy by the still in the form of latent heat of evaporation to the ambient via condensation of the water vapor on the relatively cooler inner surface of the glazing (i e, less than 10% of the thermal energy is utilized to raise the still basin water temperature) Multiple-effect solar stills are designed to recycle the latent heat of condensation to heat or pre-heat the still basin temperature

A number of manuscripts have been published which describe and/or model multiple-effect solar stills in which an air stream moves above a water film or utilize forced convection techniques A significant enhancement still productivity has been reported for these modified solar stills Yeh (1985, 1995) modified Lof's equations to derive energy balance equations to model an upward-type, double-effect solar still with air flow through the second-effect unit Thomas et al (1990) developed a model to describe a ventilated solar evaporator with convective air flow for enhanced evaporation A solar still utilizing an air stream in the evaporative channel, vaporizing the water by forced convection and condensing it on an external condenser is described by Assouad and Lavan (1988) Rahim (1995) describes a forced condensation technique as a applied to a moving water film on a tilted solar still, where the evaporator and condenser are two separate units Such a design makes it possible to increase the temperature difference between the two units

The heat and mass transfer for liquid evaporation into an air stream has been studied extensively Smolsky and Sergeyev (1962) found that there is considerable increase in heat and mass transfer due to the air stream This enhancement was explained as being the result of the evaporation of fine water droplets carried away by the air stream from the wetting surface into the boundary layer

Mink et al (1993, 1995) and Aboabboud (1997) have recently described the performance and analysis of a forced convection, multiple-effect solar still These studies have indicated that the proposed design has the still productivity

We will present two mathematical models that have been developed, independently, to describe the heat and mass transfer processes occurring in an air-blown, multiple-effect solar still with thermal energy recycle as designed by Mink et al (1993, 1995) and Aboabboud (1997) Both models utilize non-linear differential equations to describe the system under both transient and steady-state conditions The primary aim of this

study was to use an accurate as possible simulation procedure so as to appraise and quantify each of the forced multi-flow effects Nevertheless, sufficiently simple numerical procedures were adapted to the form of the physical system under consideration These models were validated by a detailed comparative analysis of their predictive ability utilizing experimental measurements on such a solar still The still being developed under a joint Israeli-Hungarian research program, will be described briefly in the following section, since a companion paper describing in detail its operation and experimental results will be presented separately (Mink et al (1997)

2 SOLAR STILL DESCRIPTION

The air-blown, multiple-effect solar still is essentially of the tilted-wick genre in the form of a thin rectangular box divided into two chambers by a central metal sheet A slot between the two chambers at the top of the tilted still allows for passage of the air stream from the upper to lower chamber The upper chamber functions as an evaporator and the lower as a condenser and it operates in the following manner (i) ambient air is drawn into the upper chamber (via a blower attached to the exit from the lower chamber) from the lower end of the tilted still, which is provided with a series of air-inlet holes, and sweeps the water evaporated from the tilted wick into the lower chamber, (ii) the major portion of the water vapor condenses either on the backside of the metal sheet, which serves both to separate the two chambers and supports the wick, or on the serpentine tube, attached to the backside of the metal sheet, transporting the feedstock to the upper chamber, (iii) the serpentine tube enters the upper chamber, via the slot, and releases the feedstock at the top edge of the metal sheet which has a weir to facilitate even wetting of the tilted wick (iv) the distillate is collected by draining from the lower chamber into a collection vessel, (v) the saturated air stream exiting the lower chamber enters an external condenser to recover water vapor prior to venting to the ambient via the blower A schematic diagram of the solar still is shown in Fig 1 It should be noted that the still glazing does not function as a condensation surface and therefore it is possible and recommended to utilize a double glazing even non-wetting polymeric glazings, to reduce the thermal energy losses through the glazing to the ambient

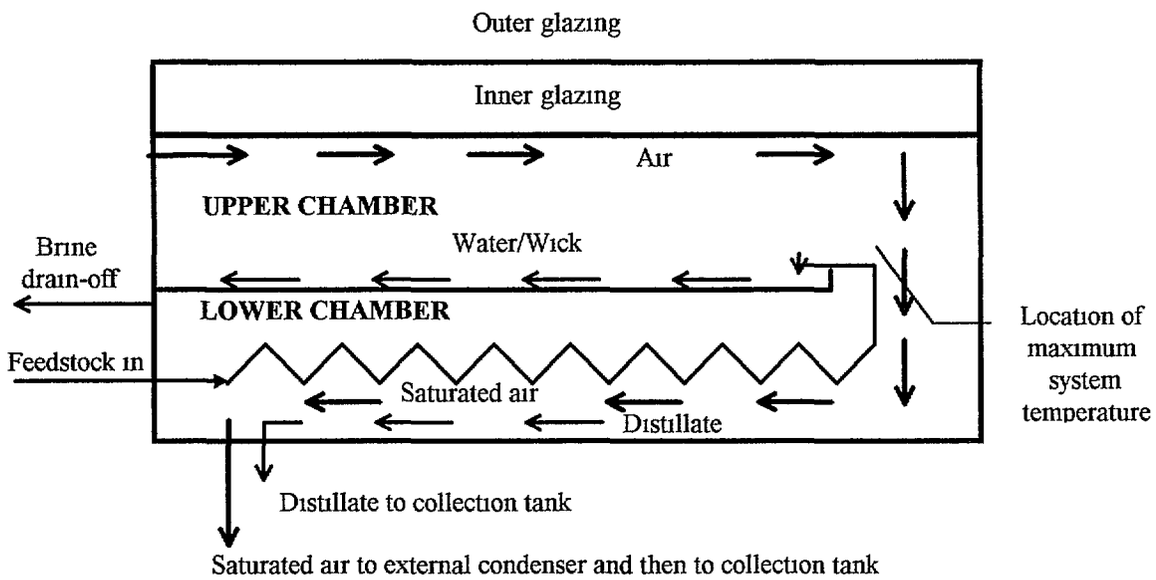

Fig 1 Schematic diagram of air-blown, multiple-effect solar still with thermal energy recycle

3 MATHEMATICAL MODEL

As mentioned above, the scientists at the both institutions (Ben-Gurion University, BGU, and the Research Laboratory for Inorganic Chemistry, RLIC) have developed, independently mathematical models to describe the heat and mass transfer processes occurring in the proposed solar still design Both models utilize non-linear differential equations to describe the system under transient and steady-state conditions The models predict both air and water stream temperatures, water vapor content of the air stream and distillate rate The two groups differ in their approach to the solution of the non-linear differential equations and the major differences between their respective solutions are the following

a RLIC utilize an approximate exponential correlation between enthalpy and the temperature of the air/water vapor stream found to be valid in 40 to 85^{0}C range typical for such solar still systems This converts

the non-linear differential equations, which do not have analytical solutions, into differential equations with simple exponential coefficients BGU applies numerical integration to solve the non-linear differential equations

b In order to reduce the number of variables, RLIC assumes that at any cross-section of the still the temperatures of the water film on the wick serpentine tube, metal sheet and saturated air stream in the upper chamber are approximately of equal value and similarly for the condensed water and the saturated air stream in the lower chamber Such approximations appear to be reasonable in view of the relatively small spacing dimensions in the two chambers (viz , the spacing between the metal sheet and the inner glazing/backside are < 15 mm) BGU assumes only that the temperatures of the water film on the wick and the metal sheet are the same

c RLIC determines the water vapor content of the air stream using the exponential correlation described above, whereas BGU utilizes a differential temperature equation

d RLIC assumes that the upper and lower chamber air streams are saturated throughout and BGU assumes that only the air stream layer in contact with the water/wick interface in the upper chamber and the air stream layer in contact with the metal sheet/serpentine tube in the lower chamber are saturated

e RLIC determines the distillation rate from the water vapor content as calculated using the abovementioned exponential correlation BGU applies the heat and mass transfer analogy to determine the forced convective mass transfer, using the air and water temperatures, and thereby the distillation rate

BGU Model

Initially, two different numerical modeling methods were tested to determine which gave better agreement with the experimental data A 'running count' technique using iterative calculations of the non-linear coefficients at each time interval and non-iterative two-stage 'predictor-corrector technique The first method was found to be more suitable for the modeling of the solar still and will be used exclusively in this study

The following assumptions were made in the analysis

1 The salt concentration of the feedstock is assumed to be sufficiently low and is neglected in the analysis

2 The system is considered uni-directional in the direction of flow for the individual streams

3 The thermal properties of the system are assumed to be independent of temperature

4 The temperature of the water film on the tilted wick is assumed to be at the same temperature as the metal sheet supporting the wick

5 Only the transverse conductivity through the glazing, metal sheet and serpentine tube are considered

The solar still shown schematically in Fig 1 was modeled by means of six non-linear differential equations These equations, incorporating the above listed assumptions, are as follows

A Upper chamber thermal energy balances ($0 < x < L_u$)

i Still glazing

$$\rho_g \delta_g c_g \partial T_g/\partial t = (\tau\alpha) G(t) + h_u (T_u - T_g) + h_{amb} (T_{amb} - T_g) + \varepsilon_p \sigma (T_p^4 - T_g^4) + \varepsilon_g \sigma (T_{sky}^4 - T_g^4) \quad (1)$$

ii Air stream

$$c_u (m_u + m_e) (v_u^{-1} \partial T_u/\partial t + \partial T_u/\partial x) = W_u [h_u(T_g - T_u) + (h_u + A_t A_u^{-1} h_c) (T_p - T_u)] + \lambda(T_u) m_e L_u^{-1}, \quad (2)$$

iii Central metal sheet (plate) with water flowing down wick

$$(m_w - m_e) [(c_w + c_p) v_w^{-1} \partial T_p/\partial t - c_w \partial T_p/\partial x] = W_u[(\tau\alpha) G(t) + (h_u + A_t A_u^{-1} h_c) (T_u - T_p) + U_{pt} (T_t - T_p) + U_{pl} (T_l - T_p) + \varepsilon_p \sigma (T_g^4 - T_p^4)] - \lambda(T_p) m_e L_u^{-1} \quad (3)$$

B Lower chamber thermal energy balances ($0 < x' < L_l$)

i Air stream

$$c_l (m_u + m_e - m_c) (v_l^{-1} \partial T_l/\partial t - \partial T_l/\partial x') = W_l (U_{pl} (T_p - T_l) + (h_l + A_t A_g^{-1} h_c) (T_t - T_l) + U_{amb} (T_{amb} - T_l) - \lambda(T_l) m_c L_l^{-1} \quad (4)$$

ii Feedstock flowing through serpentine tube

$$\pi r_i^2 \rho_f c_f \partial T_f/\partial t + m_f c_f \partial T_f/\partial x' = 2 \pi r_o U_{tf} (T_t - T_f), \quad (5)$$

iii Serpentine tube

$$(r_o^2 - r_i^2) \rho_t c_t \partial T_t/\partial t = U_{tf} r_o (T_f - T_t) + (2 \pi)^{-1} W_l [h_c (T_l - T_t) + U_{pt} (T_p - T_t)] + \lambda(T_t) m_c L_l^{-1} \quad (6)$$

The time-dependent terms in Eqs 1 through 6 refer to the rate of thermal energy transfer from the following control volumes $W_u\ \delta_g\ \Delta(x)$, $D_{hu}\ W_u\ \Delta(x)$, $(\delta_p + \delta_{wick})\ W_u\ \Delta(x)$, $D_{hl}\ W_l\ \Delta(x)$, $\pi\ r_i^2\ \Delta(x)$, $\pi\ (r_o^2 - r_i^2)\ \Delta(x)$, respectively

C The above equations were solved by imposing the following initial and boundary conditions

$$T_u\ (x,0) = T_l\ (x',0) = T_{air} \tag{7-a}$$
$$T_f\ (x',0) = T_p\ (x,0) = T_{fi} \tag{7-b}$$
$$T_g\ (0) = T_{air} \tag{7-c}$$
$$T_t\ (0) = T_{fi} \tag{7-d}$$
$$T_u\ (0,t) = T_{air} \tag{7-e}$$
$$T_f\ (0,t) = T_{fi} \tag{7-f}$$

The temperature of the air stream exiting the upper chamber, reversing its flow direction, and entering the lower chamber is assumed to be unchanged in the vicinity of the slot, viz ,

$$T_u\ (x,t)_{at\ x=L} = T_l\ (x',t)_{at\ x=L}, \tag{8}$$

and the temperature of the central metal sheet at its upper extremety is assumed to equal to that of the feedstock being discharged there from the serpentine tube, viz ,

$$T_p\ (x,t)_{at\ x=L} = T_f\ (x',t)_{at\ x=L} \tag{9}$$

The individual heat transfer coefficients as applied to each specific heat transfer process were determined from the appropriate correlations available in the literature in terms of the Nusselt number Similarly, the mass transfer coefficients for evaporation and condensation were determined from the Sherwood number correlations applicable to the mass transfer processes occurring in the solar still module The six equations governing the heat transfer processes occurring within the solar still were then solved by the numerical method described above

RLIC Model

It is apparent from the description of the approach used by each of the two groups to solve the non-linear differential equations simulating the solar still, that the RLIC model is the more simplified method They utilized the Runge-Kutta method for the solution of the differential equations, which constituted their simplified model, to simulate solar still performance The differential equations utilized in this model are as follows

A Upper chamber thermal energy balance

The following heat transfer processes contribute to the enthalpy balance on the air-vapor mixture flowing, in the upward direction, in the upper chamber (i) solar radiation absorbed, (ii) the thermal energy recycled from the lower chamber via the central metal sheet, (iii) thermal energy transferred to water/feedstock flowing down the tilted wick, (iv) thermal energy losses to ambient via the still glazing, (v) thermal energy losses via the perimeter of the upper chamber casing to both the ambient and to the lower chamber The differential equations describing the heat transfer process occurring in the upper chamber, the last factor has been neglected since the perimeter area is relatively small and insulated, are

$$V_a\ dQ_u/dA = G_{abs} + q_R + c_w\ (m_w\ dT_p/dA + T_p\ dm_w/dA) - U_{p\ amb}\ (T_p - T_{amb}), \tag{10}$$

and the water flow rate of at any cross section is is given by

$$m_w(i+1) = m_w(i) + V_a\ [H_v(i+1) - H_v(i)] \tag{11}$$

In the above analysis Q_u is defined as the enthalpy of the saturated air stream flowing through the upper chamber, i e , for the case of a unit volume of dry air at STP is saturated at T_u (1 1845 kg air), and H_v is the equilibrium humidity in kg water per m^3 dry air

B Lower chamber thermal energy balances

The air stream exits the upper chamber at the slot connecting the two chambers and reverses its flow direction upon entering the lower chamber and flows toward the outlet from the lower chamber at the bottom of the tilted still In the lower chamber the saturated air stream condenses and the mixture of saturated air and condensate is characterized by monotonic decrease in both temperature and enthalpy The rate of change of the mixture enthalpy with lower chamber area, dQ_l/dA, is positive, since the area of the lower chamber is considered to increase in the direction opposite to the flow direction of the mixture In the lower chamber the following heat transfer processes contribute to the enthalpy balance on air-vapor mixture flowing in the lower

chamber (i) thermal energy transferred to the central metal sheet by condensation from the air stream, (ii) thermal energy transferred to the serpentine tube to preheat the feedstock, (iii) thermal energy losses by conduction through the back and side walls (both are insulated) of the solar still, (iv) enthaply of condensation (v) thermal energy losses via the perimeter of the lower chamber casing The differential equations describing the heat transfer process occurring in the lower chamber, once again the last factor has been neglected, are

$$V_a\, dQ_l/dA = q_R + q_{Rp} + U_{b\,amb}\,(T_l - T_{amb}) + dq_c/dA, \tag{12}$$

where the differential thermal energy of condensation released in the lower chamber, dq_c/dA, is

$$dq_c/dA = c_w\, m_c\, dT_l/dA + c_w\, T_l\, dm_c/dA, \tag{13}$$

and the condensate flow rate of at any cross section is given by

$$m_c(i) = m_c(i+1) + V_a\,[H_v(i+1) - H_v(i)] \tag{14}$$

C Solution of the differential equations

Approximate exponential correlations for both the enthalpy and the humidity of the air/water vapor mixture as a function its temperature were developed from the thermodynamic properties of the mixture data fitting, and are given by

$$Q = \alpha_Q\, e^{\beta T}, \tag{15-a}$$

$$H_v = \alpha_H\, e^{\beta T}, \tag{15-b}$$

where α_Q = 12807 J m^{3}, α_H = 0 0048 kg m^{3}, β = 0 0617 ^{0}C^{1} (applies to both equations and note that the temperature T is in ^{0}C) The rate of change of the mixture enthalpy and humidity with chamber area is then

$$dQ/dA = \alpha_Q\, \beta\, e^{\beta T}\, dT/dA, \tag{16-a}$$

$$dH_v/dA = \alpha_H\, \beta\, e^{\beta T}\, dT/dA \tag{16-b}$$

Substituting Eqs (16-a), (16-b) into (10) gives the following

$$dT'_u/dA = U_{p\,amb}\,(C_3 - T_u)/[V_a\, \alpha_Q\, \beta\, e^{\beta T_u} - c_w\,(m_w + T'_u\, V_a\, \alpha_H\, \beta\, e^{\beta T_u})], \tag{17}$$

where C_3 is defined as

$$C_3 = (G_{abs} + U_{p\,amb}\, T'_{amb} + q_R)/U_{p\,amb} \tag{18}$$

A material balance on the water stream in the upper chamber gives the following result

$$dm_w/dA = V_a\, dH_v/dA, \tag{19}$$

and from Eq (16-b)

$$dH_v/dA = \alpha_H\, \beta\, e^{\beta T_u}\, dT'_u/dA, \tag{20}$$

and the combination of the above two equations gives

$$dm_w/dA = V_a\, \alpha_H\, \beta e^{\beta T_u} dT'_u/dA \tag{21}$$

The combination of Eqs (17) and (20) gives

$$dm_w/dA = U_{p\,amb}\,(C_3 - T'_u)(V_a\, \beta\, \alpha_H\, e^{\beta T_u})/[V_a\, \alpha_Q\, \beta\, e^{\beta T_u} - c_w\,(m_w + T'_u\, V_a\, \alpha_H\, \beta\, e^{\beta T_u})] \tag{22}$$

The differential Eqs (17) and (20) are solved numerically as functions of the still area (viz, the stream location within the solar still) for a range of air flow rates and thermal energy recycle values using Runge-Kutta method

4 RESULTS

BGU Model

The BGU model was first validated by simulating the performance of the prototype RLIC-1 solar still module, which had a solar still area of 0 24 m^2 and was double glazed (3 mm thick glass) The comparison of the experimentally measured and simulating air/water vapor mixture and water/feedstock temperatures is reported in Table 1 The still operated under the following conditions m_w = 0 452 kg h^{1}, v_{air} = 0 12 m s^{1} and G = 650 W m^{2} It is observed from Table 1 that the BGU model does a satisfactory description of the solar still

performance It predicts somewhat lower temperatures for the air/water vapor stream in the upper chamber but closely simulates still performance, with regard to the air/water vapor stream, in the lower chamber The results with regard to the temperatures of the water/feedstock flowing through the serpentine tube and its outlet onto the upper extremity of the metal sheet in the upper chamber, are reasonable except for the relatively large discrepancy for the latter

Table 1 The comparison of simulated (BGU model) air-water vapor mixture and water/feedstock temperatures to values measured on Aug 8, 1993 for a 0 24 m^2 solar still module, RLIC-1, under the following operating conditions $m_w = 0\ 452\ kg\ h^{-1}$, $v_{air} = 0\ 12\ m\ s^{-1}$ and $G = 650\ W\ m^{-2}$

Air-water vapor	$T_u(\Delta x)$ (°C)	$T_u(L/2)$ (°C)	$T_u(L - \Delta x)$ (°C)	$T_l(L - \Delta x)$ (°C)	$T_l(L/2)$ (°C)	$T_l(\Delta x)$ (°C)
RLIC-1 meas	54 1	70 4	75 7	74 0	71 1	58 9
Dew point	-	63 6	69 1*	69 1*	69 1*	58 9
BGU model	45 4	65 3	69 2	69 2	70 1	60 5
Water/feedstock	$T_f(\Delta x)$ (°C)	$T_f(L - \Delta x)$ (°C)	$T_w(\Delta x)$ (°C)			
RLIC-1 meas	42 3	73 5	51 4			
BGU model	46 5	70 2	60 2			

* Dew Point refers to relative humidity of 0 86 as determined from the mass balance on the solar still

Note Δx refers to a single increment after entering the tilted still as measured from the bottom and $(L - \Delta x)$ refers a site one increment below the upper extremity of the central metal plate

RLIC Model

The results from the RLIC model applied to a double-glazed (3 mm thick glass) solar still as a function its length are reported in Table 2 The operating conditions are assumed to be as follows $G_{abs} = 350\ W\ m^{-2}$, $V_a = 2\ 5\ m^3\ h^{-1}$ and $q_R = 400\ W\ m^{-2}$ It is possible by interpolation from Table 2, to predict the performance of the solar still module tested at RLIC, which has a length of 1 85 m (still area = 1 m^2) This results in a total amount of water vapor carried by air stream equal to 1 348 kg/h, and a net amount of water vapor evaporated in the still equal 1 240 kg h^{-1}, which is in good agreement with the experimental results

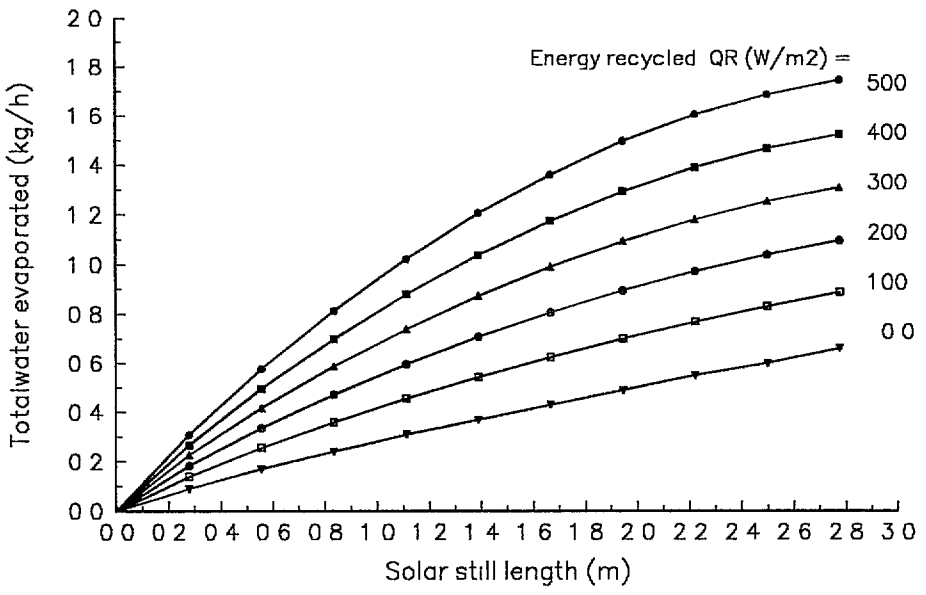

Fig 2 Total net water evaporated and removed from a double-glazed solar still by the exiting air stream as a function of both the solar still length and thermal energy recycled from the lower to upper chamber under the following conditions $G_{abs} = 350\ W\ m^{-2}$, $V_a = 2\ 5\ m^3\ h^{-1}$

The calculated total net water evaporated and removed from the still by the exiting air stream as a function of both the solar still length and thermal energy recycled from the lower to upper chamber is presented Fig 2 under the following conditions G_{abs} = 350 W m^{2}, V_a = 2 5 m^3 h^{1} In Fig 3 the calculated air/water vapor temperature as a function of both the solar still length and thermal energy recycled from the lower to upper chamber is shown under the same operating conditions

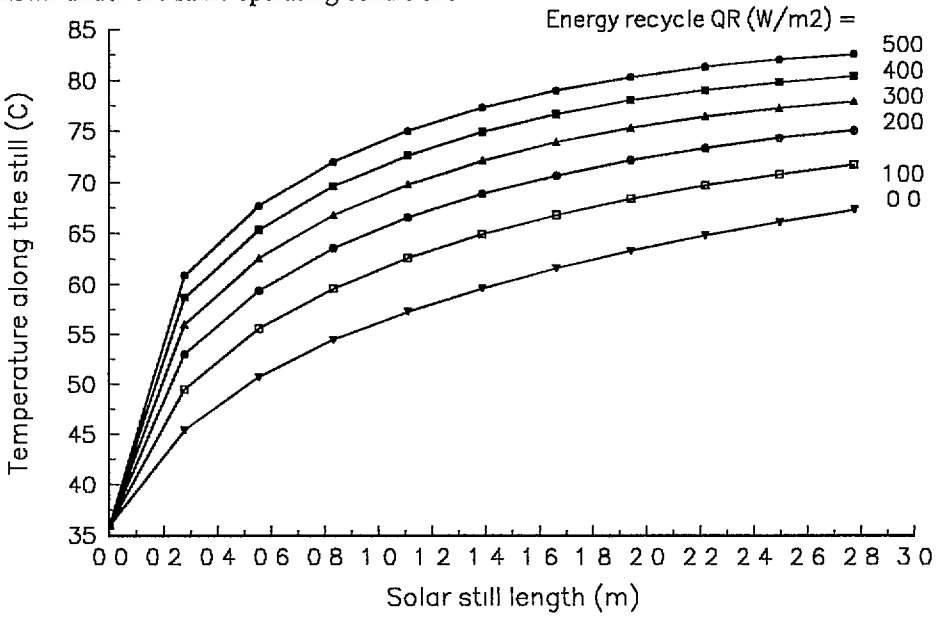

Fig 3 Variation of the air/water vapor mixture temperature in a double-glazed solar still with still length and thermal energy recycle rate under the following conditions G_{abs} = 350 W m^{2}, V_a = 2 5 m^3 h^{1}

The variation in the air/water vapor mixture enthalpy with solar still length for G_{abs} = 350 W m^{2}, V_a = 2 5 m^3 h^{1} and q_R = 400 W m^{2} is shown in Fig 4 In Fig 5 the variation in air/water vapor mixture temperature as a function of both solar still length and air flow rate is shown under the following conditions G_{abs} = 350 W m^{2} and q_R = 400 W m^{2}

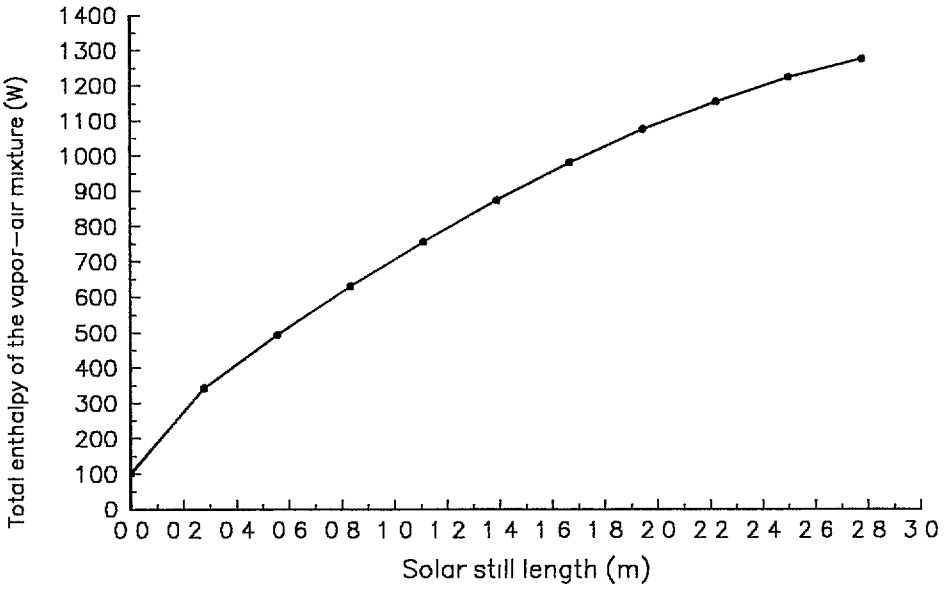

Fig 4 Variation of the air/water vapor mixture enthalpy in a double-glazed solar with still length under the following conditions G_{abs} = 350 W m^{2}, V_a = 2 5 m^3 h^{1} and q_R = 400 W m^{2}

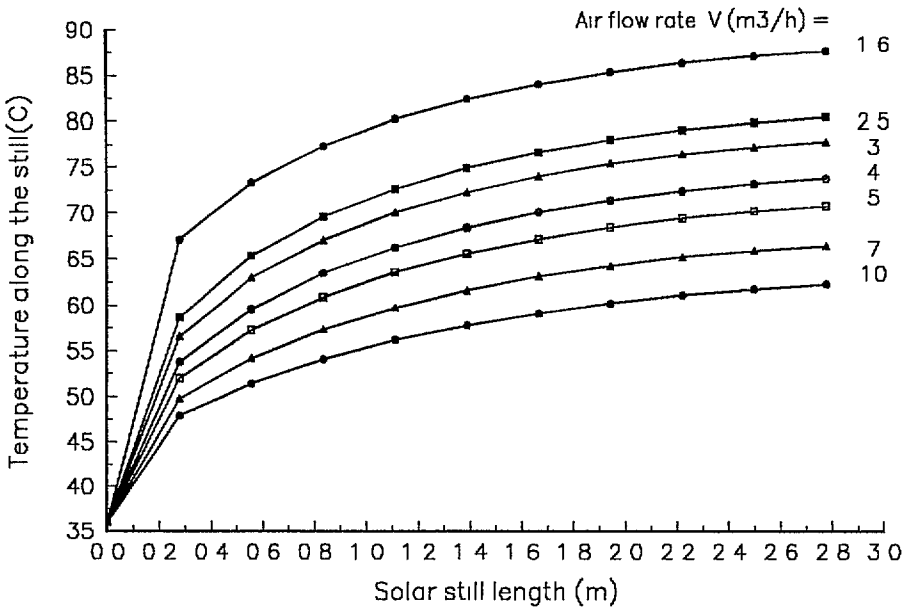

Fig 5 Variation of the air/water vapor mixture temperature in a double-glazed solar still as a function of both still length and air flow rate under the following conditions G_{abs} = 350 W m^{2} and q_R = 400 W m^{2}

Table 2 The calculated (RLIC model) air/water vapor mixture temperature T'_u, total mass flow rate of vapor $V_a H_v$, thermal energy flow rate $V_a Q_u$, net amount of water vapor in air stream, water/feedstock flow rate and net water evaporated as a function of still length Amount of water vapor entering with ambient air is 0 108 kg h^{1}, and the brine drain-off flow rate is 1 2 kg h^{1}

Still length (m)	T_u (°C)	$V_a H_v$ (kg h^{1})	$V_a Q_u$ (W)	Net vapor in air (kg h^{1})	Brine flow rate (kg h^{1})	Water evaporated (kg h^{1})
0 0	35	0 108	101 3	0 000	1 200	0 000
0 28	58 7	0 417	343 1	0 309	1 466	0 266
0 56	65 4	0 615	493 8	0 507	1 695	0495
0 83	69 6	0 796	630 5	0 6885	1 898	0 698
1 11	72 6	0 964	756 8	0 8564	2 079	0 879
1 39	74 9	1 121	874 3	1 0128	2 238	1 038
1 67	76 6	1 264	981 5	1 1558	2 377	1 177
1 94	78 0	1 390	1076 5	1 2825	2 494	1 294
2 22	79 0	1 496	1155 7	1 3882	2 592	1 392
2 50	79 8	1 588	1224 9	1 4806	2 669	1 447
2 78	80 4	1 658	1276 8	1 5499	2 727	1 526

BGU and RLIC models- comparative analysis

The comparative analysis of the two models was performed using the data measured on RLIC-2 a 1 m^2 solar still module The measured and simulated values for the air/water vapor mixture in the upper chamber as a function of still length are reported in Table 3 The temperature values listed for RLIC-2 were obtained from the experimental data by interpolation to the corresponding still lengths listed in Table 3 It is observed that both models somewhat underestimate the corresponding experimental values but they both predict similar trends It is also observed that the BGU model describes both the initial development of the temperature profile and the effect of the introduction of the water/feedstock at the upper extremity of the central metal sheet cf temperature values between 1 6 and 1 85 m

5 CONCLUSIONS

Two mathematical models have been developed independently by the two the groups involved in a joint research program to describe the heat and mass transfer processes occurring in an air-blown, multiple-effect solar still with thermal energy recycle

A comparative analysis, utilizing experimentally measured data on two solar still modules, has shown that both models are able to simulate the heat transfer processes occurring in the solar still modules satisfactorily however, both underestimate the steady state temperatures in the upper chamber

Table 3 The comparison of air-water vapor mixture temperature values measured in the upper chamber of a 1 m^2 solar still module, RLIC-2, as a function of still length to those simulated by both the BGU and RLIC models, under the following operating conditions $m_w = 2\ 5\ kg\ h^{1}$, $v_{air} = 0\ 12\ m\ s^{1}$, $G = 650\ W\ m^{2}$

Still length, m	0	0 2	0 5	0 8	1 1	1 4	1 6	1 8
Temperature of air/water vapor mixture in upper chamber (^{0}C)								
RLIC-2 meas	40 5	60 5	73 5	80 5	82 0	83 5	83 5	82 5
Dew point	-	53 2	66 5	73 7	75 5	77 0	77 0	76 0*
BGU model	35 0	59 5	68 7	72 6	74 3	75 0	75 1	73 4
RLIC model	35 0	58 7	65 3	69 6	72 6	74 9	76 6	78 0

* Dew Point refers to relative humidity of 0 86, as determined from the mass balance on the solar still

The BGU model predicts the local decrease in the upper chamber air/water vapor mixture temperature in the vicinity of the feedstock inlet onto the central metal plate, i e, at the upper extremity of the plate in agreement with experimental observations The RLIC model does not detect this local temperature decrease

A major difference between the two models is in their treatment of the rate of thermal energy recycle from the lower to the upper chamber, q_R The RLIC model utilizes the rate of thermal energy recycle as an iterative parameter in the solution of their differential equations The BGU model has the advantage in that it is able to calculate q_R from the initial and boundary conditions The thermal energy recycle is calculated by both models to be $\approx 400\ W\ m^{2}$ for an incident solar radiation intensity of $650\ W\ m^{2}$, in good agreement with the experimental results

We plan to continue to fine-tune the models, utilizing the experimental data measured on the solar still modules and, thereby improve their ability to simulate the solar stills

NOMENCLATURE

- A area of solar still, m^2
- c heat capacity, $J\ kg^{1}\ K^{1}$
- G incident solar radiation intensity, $W\ m^{2}$
- G_{abs} solar energy absorbed by the still, $W\ m^{2}$
- H_v equilibrium air humidity, kg water m^3 dry air
- h heat transfer coefficient, $W\ m^{2}\ K^{1}$
- L length of chamber, m
- m the mass flow rate, $kg\ s^{1}$
- Q enthalpy saturated air stream, $J\ m^{3}$
- q_c thermal energy released by condensate in lower chamber, $W\ m^{2}$
- q_R thermal energy recycled from lower chamber to upper cavity, $W\ m^{2}$
- q_{Rp} thermal energy recycled from lower chamber to central metal sheet, $W\ m^{2}$
- q_{Rt} thermal energy recycled from lower chamber to serpentine tube to preheat the feedstock, $W\ m^{2}$
- r_i inner radius of serpentine tube, m
- r_o outer radius of serpentine tube, m
- T temperature, K
- T temperature, ^{0}C
- T_{sky} sky temperature, K
- U overall heat transfer coefficient, $W\ m^{2}\ K^{1}$
- V_a volumetric flow rate of bone dry air at STP, $m^3\ s^{1}$
- v linear velocity, $m\ s^{1}$
- W width of chamber, m

Greek letters

- α_H pre-exponential in Eq (15-b)
- α_Q pre-exponential in Eq (15-a)
- β exponential in Eq (15)
- δ thickness, m

ε emittance
λ enthalpy of vaporization, J kg^{1}
ρ density, kg m^{3}
σ Stefan-Boltzmann constant W m^{2} K^{-4}
$(\tau\alpha)$ transmittance-absorptance product

Subscripts

air ambient air entering the solar stilll
amb ambient
b backside
c condensate
e evaporation
f feedstock in serpentine tube
fi inlet feedstock
g glazing
l lower chamber
p plate (i e , central metal sheet)
t serpentine tube
u upper chamber
w water (feedstock on wick)

Acknowledgment- This research was supported under Grant No TA-MOU-95-C15-050, US-Israel Cooperative Development Research Program, Office of Agriculture & Food Security, Center for Economic Growth, Bureau for Global Programs, Field Support and Research, USAID

REFERENCES

Aboabboud, M M (1997) Design and investigation of a new, air-blown solar still with internal energy recycle PhD Thesis, Research Laboratory for Inorganic Chemistry, Hungarian Academy of Sciences, Budapest Hungary

Assouad, Y and Lavan, Z (1988) Solar desalination with latent heat recovery *J Solar Energy Engineering* **110,** 14-16

Delyannis, A and Delyannis, E E (1980) *Seawater and Desalting*, Vol 1 pp 67-70, Springer-Verlag, Berlin

Duffie, J A and Beckman, W A (1980) *Solar Engineering of Thermal Processes*, Wiley Interscience New York

Kudish, A I (1991) Water Desalination In *Solar Energy in Agriculture-Energy in World Agriculture* Parker B F (Ed), Vol 4, pp 255-294 Elsevier Science Publishers B V Amsterdam

Malik, M A S , Tiwari, G N , Kumar, A and Sodha, M S (1982) *Solar Distillation* Pergamon Press, Oxford

Mink, G Aboabboud, M M and Karmazsin, E (1993) Solar still of improved efficiency In *Proceedings of ISES Solar World Congress,* Budapest, p 319

Mink G Aboabboud, A A , Horvath, L , Evseev, E G and Kudish, A I (1997) Design and performance of an air-blown, multiple-effect solar still with thermal energy recycle, submitted to Solar Means Business , 1997 ISES Solar World Congress, Korea

Mink, G , Karmazsin, E , Yasin, M , Aboabboud, M M , Horvath, L and Kudish, A I (1995) Energy recycling in air-blown solar stills In *Proceedings and Abstracts Sixth ASEAN Conference on Energy Technology*, Bangkok, Thailand, p 442

Rahim, N A (1995) Utilization of forced condensing technique in moving film inclined solar still *Desalination* **101,** 255-262

Smolsky, B M and Sergeyev, G T (1962) Heat and mass transfer with liquid evaporation *Int l J Heat Mass Transfer* **5,** 1011-1021

Thomas D L , Guinn G R and Thomason, B O (1990) Analysis of ventilated solar evaporator for concentrating dilute hazardous waste *Solar Energy* **45,** 101-104

Yeh, H M and Chen L C (1985) Basin-type solar distillation with air flow through the still *Energy* **10,** 1237-1241

Yeh, H M and Chen, Z F (1994) Energy balances for upward-type, double-effect solar distillers with air flow through the second-effect unit *Energy* **19,** 619-626

Submitted to *Solar Energy* (Oct 28, 1997)

DESIGN PARAMETERS, PERFORMANCE TESTING AND ANALYSIS OF A DOUBLE-GLAZED, AIR-BLOWN SOLAR STILL WITH THERMAL ENERGY RECYCLE

G MINK[*1], L HORVATH[*], E G EVSEEV[**] and A I KUDISH[**12]

[*]Research Laboratory for Inorganic Chemistry, Hungarian Academy of Sciences, 1518 Budapest Pf 132, HUNGARY, Tel +36 1 3193119, Fax +36 1 3192537,

E-mail mink@sparc core hu

[**]Solar Energy Laboratory, Department of Chemical Engineering, Ben-Gurion University of the Negev, Beer Sheva 84105, ISRAEL , Tel +972 7 6461488, Fax +972 7 6472916,

E-mail akudish@bgumail bgu ac il

[1] Member of ISES
[2] Author to whom all correspondence should be addresses

Abstract - An air-blown, multiple-effect solar still with thermal energy recycle consisting of an upper evaporation chamber and lower condensation chamber, the prototype originally proposed by the scientist at the Research Laboratory for Inorganic Chemistry (Mink et al 1988), is being developed and tested under a joint Israeli-Hungarian research program The principle of operation of such a still, the main design parameters and the results of solar still performance tests will be presented The present discussion will be restricted to the performance testing of a solar still with a nominal still area of 1 m^2 (1 86 m x 0 54 m) utilizing a solar simulator providing a constant radiation intensity of 630±39 Wm^{2} The solar still performance was monitored under the following conditions constant feedstock flow rate, 2 96 $kgm^{2}h^{1}$, and varying air flow rate, in the range from 0 32 to 4 51 $kgm^{2}h^{1}$ It was observed, under these conditions, that the thermal energy recycle began to be effective after about 30 minutes and that the still achieved steady-state after approximately one hour of operation The steady-state distillation rate exhibits an optimum (of the order of 1 1 $kgm^{2}h^{1}$) for an air flow rate in the range from 1 02 to 1 24 $kgm^{2}h^{1}$ The experimental results indicate that the still performance can be enhanced further by increasing the linear air stream velocity in the lower chamber by decreasing its cross sectional flow area

32

1 INTRODUCTION

Today there exists an estimated two billion people who go without fresh water on a daily basis The consumption of water unfit for drinking, due to pathogens and salinity, is a major health hazard world-wide In addition, the growth of the world's population and the consequent food shortage, requires the expansion of agriculture into arid zones, i e , the greening of the desert The famine in the Sahal region (viz , the Sahara Desert) and other less publicized regions on the globe provide ample evidence for the necessity of solving this problem by concerted efforts, both national and international Arid zones constitute 60% of the earth's land area and they are, in general, characterized by high levels of solar radiation and shortages of fresh water Such regions often possess reservoirs of either brackish or saline water that may be used for both drinking and irrigation after suitable treatment Solar desalination systems may be an ideal source of fresh water for both drinking and agriculture in arid zones This is especially true in that both the demand for fresh water and the intensity of solar radiation are, in general, cyclical in nature and in phase with each other

The utilization of solar energy for the distillation of brackish or saline water has been practiced for a very long time Various types of solar stills and solar-assisted desalination units have been designed and investigated A number of manuscripts have been published on this subject a classic one by Talbert et al (1970) and two more recent ones by Malik et al (1982) and Kudish (1991) The main disadvantage of most solar stills is their inherent relatively low efficiency, viz , their efficiency, notwithstanding intensive research and development efforts, remains stalled in the 30-40% range

If we apply this finding to arid zones, which are characterized by the greatest shortages of potable water, one arrives at the following conclusion present day state-of-the-art single-effect solar stills cannot be expected to exceed an annual productivity limit of $1 m^3 m^{-2}$ This assumes that the cumulative annual global radiation incident on the Earth's surface in these arid

regions is about 8 x 10^6 $kJm^{-2}y^{-1}$ and the annual still efficiency is of the order of 30% The major drawback in the design of such single-effect solar stills is the dumping, in excess of 90%, of the solar energy converted to thermal energy, by the still in the form of latent heat of evaporation to the ambient via condensation of the water vapor on the relatively cooler inner surface of the glazing (i e , less than 10% of the thermal energy is utilized to raise the still basin water temperature, sensible heat) Multiple-effect solar stills are designed to recycle some fraction (preferably a large one) of the latent heat of condensation to heat or preheat the feedstock

In the single-effect system, the solar radiation is absorbed by an absorbing surface (e g , a black water basin liner) which converts the solar to thermal energy The basin liner (black to maximize visible radiation absorption) collects the solar radiation, since water absorbs in the infrared range of the solar spectrum and is not capable of converting the solar radiation, essentially composed of visible radiation (approximately 5% is ultraviolet and a negligible amount of infrared), directly to thermal energy The thermal energy is transmitted by convection through the water to its surface The water at the water-vapor interface evaporates and then condenses on the relatively cooler still glazing surface The latent heat of condensation is vented to the ambient in such systems during the condensation process on and via the still glazing surface It has been reported by Delyannis and Delyannis (1980) that the overall efficiency of a typical basin type solar still is usually 30% or lower This is the underlying reason for the limited use of solar desalination plants constructed from such solar stills In addition, they require the availability of large land areas and the fixed capital investment is directly proportional to the size (basin area) of the plant, though economics of scale may be involved with the peripheral equipment (mainly pumps and storage vessels, which, in general, contribute a small percentage to the total fixed capital investment) and operation and maintenance costs

The multiple-effect solar still systems are designed to recover/recycle some fraction of the latent heat of condensation to preheat the feedstock either prior to entering or within the solar still basin and thereby enhance the system efficiency This may be accomplished, in the former case, by condensing the water vapor on the surface of a heat exchanger through which the feedstock flows as the heat exchange medium For example, the still may be constructed with a double glazing and by flowing the feedstock through the space between the glazing (i e , essentially a simple liquid in glass condenser) prior to entering the still basin Such a design, obviously, necessitates operating the still as a flow system (i e , a continuous feed input) rather than a batch system It also requires leakproof sealing of the double glazing This may be facilitated by using an internally sealed doubled glazing such as that available for double glazed windows (i e , 'storm windows') but at a much greater cost than single glazings

An example of the recovery/recycle of the latent heat of condensation within the solar still system is that analyzed by Sodha et al (1980) It is designated as a double basin solar still and is a simplified version of a multiple level solar still originally proposed by Lobo and Araujo (1977) It is designed to utilize the latent heat of condensation from the lower basin (viz , the condensation of the water vapor on the underside of the transparent base supporting the upper basin) to heat the water in the upper still basin This requires the use of a transparent base (e g , glass) for the upper still The practical application of such a design is questionable due to the many technical problems involved, such as the load on the transparent base of the upper still

The two still designs described above are classified as double-effect solar stills, a single recovery/recycle of the latent heat of condensation It is possible to envision the design of multiple-effect solar stills (e g , adding on more basins with transparent bases, one top of the other, to achieve a multiple-effect) similar in concept to multiple-effect conventional desalination techniques Needless to say, the cost of the solar still construction increases with

35

complexity of the design and any additional costs must be weighed against the potential for increased productivity/efficiency

Another example of such recycle systems is that described by Kossinger et al (1993), i e , a highly efficient solar desalination unit utilizing the latent heat of condensation to preheat the feedstock prior to entering the still Engelhadt et al (1997) presented a total life cycle cost analysis for this system under different modes of operation

The rationale behind the design of our air-blown, multiple-effect solar still was to overcome the inherent disadvantage in the operation of single-effect solar stills, viz , their efficiency, notwithstanding intensive research and development efforts, has remained stalled in the 30-40% range Our goal being, enhanced productivity while incurring minimal incremental costs This air-blown, multiple-effect solar still is designed to recycle the thermal energy (i e , the latent heat of condensation), which is dumped/vented to the ambient in single-effect solar stills, to heat or preheat the feedstock to the solar still The mode of operation of this solar still will be described together with experimental results in the following sections

A number of manuscripts have been published which describe and/or model multiple-effect solar stills in which an air stream moves above a water film or utilize forced convection techniques A significant enhancement in still productivity has been reported for these modified solar stills Yeh (1985, 1995) modified Lof's equations to derive energy balance equations to model an upward-type, double-effect solar still with air flow through the second-effect unit Thomas et al (1990) developed a model to describe a ventilated solar evaporator with convective air flow for enhanced evaporation A solar still utilizing an air stream in the evaporative channel, vaporizing the water by forced convection and condensing it on an external condenser is described by Assouad and Lavan (1988) Rahim (1995) describes a forced condensation technique as a applied to a moving water film on a tilted solar still, where

the evaporator and condenser are two separate units Such a design makes it possible to increase the temperature difference between the two units

The significance of this research project is obvious in that potable water is a commodity that is becoming scarce and has been a source of conflict between nations throughout history If the latter part of the 20th Century can be characterized as one that the scarcity of oil was a casus belli than it is reasonable to state that the casus belli in the 21st Century will be the scarcity of water In fact, the success of the peace treaties now in effect and in the making in the Middle East will depend to a significant degree on the availability of water for all countries concerned Solar desalination can be an important source for water in this region, which is primarily composed of arid and desert lands and has an abundance of solar radiation

2 SOLAR STILL DESCRIPTION

A schematic diagram of the air-blown, multiple-effect solar still is presented in Fig 1 It is essentially of the tilted-wick genre in the form of a thin rectangular box divided into two chambers (upper evaporator and lower condenser) by a central metal sheet There is a slot between the two chambers at the top of the tilted still (viz , the central metal sheet does not extend across the full length of the still but leaves a slot of 10 mm between its top end and the still's upper extremity) The metal sheet also functions as (i) the support for the wick (a black porous material) which covers it on the upper chamber side, (ii) the surface to which a serpentine tube, on the lower chamber side, for transporting the feedstock to the upper chamber, is attached This serpentine tube also functions as a heat exchanger for preheating the feedstock prior to entering the upper chamber The spacing between the central metal plate and the upper chamber still glazing and the lower chamber backside are both < 15 mm

The mode of operation of the solar still is as follows (1) ambient air is pumped into the upper chamber from the bottom of the tilted still and sweeps the water vapor evaporated from the tilted wick into the lower chamber via the slot at the top of the tilted still (maximum

temperature of the air stream is measured at this point, above the slot, prior to entering to the lower chamber and serving as the hot fluid in what is essentially an air-liquid heat exchanger), (2) the major portion of the water vapor then condenses on the backside of the metal sheet supporting the wick or on the serpentine tube, which enters at the bottom of the lower chamber, transporting the feedstock to the upper chamber, (3) the feedstock, which enters the serpentine tube at a flow rate in excess of the rate of evaporation from the wick in the upper chamber and is preheated during its passage through the serpentine tube, exits the serpentine tube at the top edge of the central plate and passes over a weir and flows by gravity down the wick, (4) the distillate exits the lower chamber and is collected, whereas the saturated air stream, also exiting the lower chamber, enters an external condenser, to further condense the water vapor remaining prior to venting to the ambient

In the upper chamber the air stream flows countercurrently to the direction of feedstock flowing down the wick, whereas in the lower chamber the air stream flows both countercurrently and perpendicular to the direction of the feedstock flowing through the serpentine tube Due to the nature of this solar still, viz , that the upper chamber glazing does not serve as a condensation surface, it is possible and recommended to utilize a double glazing to reduce thermal energy losses via the glazing to the ambient In fact, it is possible to use non-wetting polymeric glazings such as those used as transparent insulating material (TIM's), e g , Qualex, a double-walled polycarbonate sheet, as the solar still glazing

3 DESIGN PARAMETERS

System design parameters

1 Feedstock and air flow rates- Previous investigations by Mink et al (1997a,b) have shown that a feedstock flow rate $m_f = 2$ kgm^{-2}h^{-1} is sufficient to completely wet the wick They also found that increasing the feedstock flow rate from 2 28 to 4 07 kgm^{-2}h^{-1} had only a negligible effect on the still productivity The present study utilized a solar still with a still area,

38

A, of 1 m^2 tilted at an angle of 20° with a constant feedstock flow rate of 2 96 $kgm^{-2}h^{-1}$ The previous investigations utilized a double glazing consisting of 3 mm glass plates with a 20 mm gap, whereas the present study utilized a double-walled polycarbonate sheet with a 10 mm gap The incident radiation intensity was 650±39 Wm^{-2}, utilizing a solar simulator Mink et al (1997a,b) found that the highest productivity was obtained for air flow rates in the range between 1 8 and 3 5 $kgm^{-2}h^{-1}$ and in the present study the air flow rates were varied between 0 32 and 4 51 $kgm^{-2}h^{-1}$

ii Utilization of the vapor content of the air stream exiting the solar still- The primary distillate via condensation in the lower chamber was estimated to be approx 0 7 $kgm^{-2}h^{-1}$ In view of the fact that the rate of evaporation in the upper chamber was found to be of the order of 1 1 $kgm^{-2}h^{-1}$, it is apparent that the saturated air stream exiting the lower chamber is also a potential source of fresh water This secondary distillate, of the order of 0 4 $kgm^{-2}h^{-1}$, can be recovered provided that the exiting air stream can be cooled by an external heat exchanger, viz , a condenser, to ambient temperature

If $H_{l,out}$ denotes the enthalpy of the saturated air exiting the lower chamber in $Jkg^{-1}{}_{BDA}$ and m_a, the mass flow rate of the air stream, is expressed in units of $kgm^{-2}s^{-1}$, the rate of thermal energy exiting with the air stream $q_{l,out}$ is given by

$$q_{l,out} = m_a H_{l,out} \qquad (1)$$

It is obvious that the temperatures within such a still are inverse functions of the mass flow rate of the air stream Consequently, it would be advantageous to operate the solar still at even lower air stream flow rates, since higher exiting air stream enthalpy values translate into both higher temperatures and partial pressures of the water vapor (or vapor content) in the exiting air stream Also, the overall heat transfer coefficient for condensation from the air stream decreases rapidly with decreasing temperature (see below) The lower air stream flow rates will result in an increase in the air stream temperature in both chambers and an increase in the

external condenser efficiency (i e , the amount of secondary distillate) as a result of the greater temperature gradient An increased condenser efficiency will allow a reduction in condenser size and/or cooling energy requirement and resultant decrease in construction and/or operating costs

As mentioned previously, an optimum air stream flow rate must exist in the range of relatively low flow rates, since for this solar still design the productivity will be zero for an air flow rate of zero Mink et al (1997a,b), based upon their experimental results and analysis, suggested that the optimum air flow rate was below the range they studied, viz , less than 1 8 $kgm^{2}h^{1}$ Consequently, in the present study the system was adapted to enable us to operate it under controllable and stable flow rates below 1 8 $kgm^{2}h^{1}$

iii Vapor/liquid separator, heat exchanger- In the performance testing of the solar still module in the laboratory it was desired to measure the primary distillation/productivity rate within the module (i e , the rate of condensation within the lower chamber, which is a direct measure of the efficiency of the thermal energy recycle process) and that obtained from the exiting air stream, secondary distillation Therefore, the vapor/liquid mixture exiting the still module first entered vapor/liquid Separator I (primary distillate), then the vapor stream was passed through a heat exchanger/condenser prior to entering vapor/liquid Separator II (secondary distillate) In a scaled-up system it would be sufficient to have the outlet vapor/liquid mixture exiting the system to pass through a heat exchanger/condenser prior to entering a single vapor/liquid separator

In the present study a simple water cooled condenser functioned as the heat exchanger but it would be very advantageous to utilize the non-negligible thermal energy present in this stream to preheat the feedstock, viz , to utilize the feedstock as the cooling medium In such a design the temperature of feedstock entering the still would approach $T_{1\,out}$ and thereby further increase

the still operating temperatures This method of operation of the solar still is discussed in detail by Aboabboud et al (1996)

iv Glazing- The amount of solar radiation absorbed within the still is the difference between the incident solar radiation G_i and the reflection losses from the still glazing G_r The utilized solar energy Q_u is determined from the difference between the solar radiation absorbed and the thermal energy losses to the ambient through the glazing $q_{loss,amb}$ Thus, the amount of utilized solar energy is given by

$$Q_u = G_i - G_r - q_{loss,amb} \quad (2)$$

The enthalpy of the air stream attains its maximum value at the top of the still, H_{max}, viz , in the vicinity of the slot connecting the upper and lower chambers, where it attains both its maximum temperature and water vapor content, is

$$m_a H_{max} = q_{max} = m_a H_{a,in} + Q_u + q_R + q_{released}, \quad (3)$$

where $H_{a,in}$ is the enthalpy of the entering air plus vapor stream in $Jkg^{-1}{}_{BDA}$, q_R is the thermal energy recycled directly to the upper chamber and $q_{released}$ is the thermal energy transferred from the preheated feedstock to the air stream It is apparent from Eqs (2) and (3) that for a given solar irradiance G, the still performance is determined mainly by the top losses $q_{loss,amb}$ and the efficiency of the thermal energy recycle processes Since the system is designed to operate at low mass flow rates of air and at relatively high temperatures, the thermal energy losses to the ambient will increase with increasing temperature To minimize these thermal energy losses the glazing should have good insulating properties This was achieved by utilizing a double glazing The disadvantage of a double glazing is the increased reflection losses, approximately an 8 % increase in reflection losses, but this is more than compensated for by the relatively higher temperature gradients, $\Delta T = T_w - T_a$, achieved In addition, since the glazing does not function as a condensation surface it was possible to use a transparent insulating material such as Qualex, a transparent double-walled polycarbonate sheet which is non-wetting, as a glazing

41

v Thermal energy recycle process and air velocity in the lower chamber- The thermal energy recycle process occurs in the lower chamber via heat transfer from the saturated air stream to the central metal plate and to the serpentine tube The rate of condensation in the lower chamber and thereby the efficiency of the thermal energy recycle is directly related to these processes The heat transfer processes include condensation and convective heat transfer from the air stream The combined heat transfer coefficient $h_{c\,g}$, which strongly depends on the temperature (the vapor content of saturated air) and its fluid mechanical properties is approximated by

$$h_{c\,g} = 1/[(1/h_c) + q_g/(q\ h_g)] \qquad (4)$$

where h_c is the heat transfer coefficient for the condensed water film, in the range of 5000 - 10000 W $m^{2}K^{1}$, h_g is the convective heat transfer coefficient of the gas film, q_g is the heat transmitted by the gas (air + non-condensing vapor) and q is the total heat transmitted

The overall heat transfer coefficient U_{lw} for thermal energy recycle process from the lower chamber to the upper surface of the wet wick, where the evaporation process is occurring, is given by

$$U_{lw} = 1/[(1/h_{c\,g}) + (1/h_m) + (1/h_{sd}) + (1/h_f) + (1/h_w)] \qquad (5)$$

where h_m is the heat transfer coefficient for the metal plate, 260 000 W $m^{2}K^{1}$ for a 1 mm thick copper sheet, h_{sd} is the heat transfer coefficient for scale deposit , approximately 5000 $Wm^{2}K^{-1}$, h_f is the heat transfer coefficient for the feedstock/brine film above the plate, about 3500 $Wm^{-2}K^{1}$ and h_w is the heat transfer coefficient for the wet wick, about 660 $Wm^{2}K^{1}$ for a 1 mm thick water film

The above equations for the heat transfer coefficients were solved by determining values for q_g/q from the Psychrometric Tables for temperature intervals of 5 °C and using the above values for the individual heat transfer coefficients The following values for the heat transfer coefficient for the gas film h_g were considered, 80, 20, 10 and 5 $Wm^{2}K^{1}$ The results of this

42

analysis are reported in Table 1 A value of h_g = 80 $Wm^{-2}K^{-1}$ corresponds to turbulent flow with Re > 10 000 and a gas velocity of 10 ms^{-1} or above, for the case of an equivalent diameter of approximately 0 02 m Using the same value for the equivalent diameter, h_g values of 20, 10 and 5 $Wm^{-2}K^{-1}$ correspond to approximately 2, 1 and 0 5 ms^{-1} gas velocities, respectively

It is obvious from the results of this analysis reported in Table 1 that the effectiveness of thermal energy recycle process and consequently the still performance depends mainly on U_{lw} It is possible to increase, to a limited extent, the value of U_{lw} by decreasing the thickness of the porous wick, cf Table 1

The results of the analysis reported in Table 1 suggest that the still should be operated at high temperatures and with high gas film heat transfer coefficient h_g values Such high temperatures can be achieved only if sufficiently low mass flow rates are applied, since at constant energy input the enthalpy gain of the air stream is inversely proportional to its mass flow rate On the other hand, high linear air stream velocities are necessary in the lower chamber in order to achieve a high heat transfer coefficient h_g This goal can be achieved by decreasing the height of the lower chamber (viz , decreasing its cross sectional flow area) and/or by accelerating the air stream velocity with the help of baffles, since the air mass flow rate must be low

In the present solar still module the feedstock is preheated in the lower chamber and its height is determined by the outer diameter of the serpentine tube Therefore, in the lower chamber the gas velocity was accelerated, by a factor of about three by means of baffles, which were concentrated in the lower temperature/section of the chamber (cf Fig 2)

vi Serpentine tube area vs still area- The ratio of the thermal energy transmitted to the serpentine tube to that directly recycled to the central plate is estimated to be in the range of 0 3 to 0 6, depending on the air stream flow rate, the temperature of the entering feedstock and the maximum temperature within the still Ideally, the ratio of the tube to plate surface area should be identical to the thermal energy recycle ratio, since the nature of heat transfer process to the

43

tube and the plate is essentially the same Nevertheless, if it is assumed that the average temperature gradient between the central metal plate and tube is $T_{m,avg} - T_{t,avg} \approx 2$ K, and considering that the overall heat transfer coefficient U_{lw} is in the range between 200 - 300 $Wm^{-2}K^{-1}$, i e , the still operates under nearly optimum condition, it is possible to reduce the tube to plate surface area ratio to about 0 2 m^2m^{-2}, in order to achieve cost savings This would be more than sufficient if the entering feedstock is preheated close to $T_{l,out}$ utilizing the enthalpy present in the air stream exiting the solar still

vii Pressure drop in the system- A drawback in increasing the air stream velocity in the lower chamber is that parasitic electric energy required to drive the air pump also increases This may be a major problem in rural application where the electric energy may be supplied by PV panels In addition, a system operating under high pressure drops requires sturdier and more expensive construction than that operating at nearly atmospheric pressure The present solar still system was designed for very low (< 100 Pa) pressure drops and may be considered to operate under atmospheric conditions

4 EXPERIMENTAL SETUP AND PROCEDURE

The solar still performance was monitored under the following conditions constant feedstock flow rate, 2 96 $kgm^{-2}h^{-1}$, and varying air flow rate, in the range from 0 32 to 4 51 $kgm^{-2}h^{-1}$ In this study the still performance was tested as a function of air flow rate only, since it had been ascertained in previous studies that the effect of feedstock flow rate on still performance is negligible (Mink et al 1997)

Experimental setup

The experimental setup (cf Fig 1) consists of the following solar still module, solar simulator, two vapor/liquid separators for collecting the product, heat exchanger, peristaltic pump to transport the feedstock, low pressure adjustable flow rate air pump, electric balance to measure distillate, gas flow meter, magnetic valves (Mv) to drain the separators periodically, electric

44

balance to measure the amount of the drained distillate and temperature sensors The system is connected on-line to a personal computer for data collection and analysis The position of the air pump ensures that the system operates at a pressure somewhat below ambient

Solar still module

The still consists of two shallow trays, supplied with perimeter rims, of slightly different dimension (cf Table 2) such that the upper tray can be inserted into the lower tray Air tightness was ensured by inserting a rubber gasket tape between the rims and between the upper rim and glazing The two trays and glazing were clamped together by screws The upper and lower trays were constructed from a 1 mm thick copper sheet and the lower tray was insulated externally (i e , its bottom and perimeter) with 50 mm thick polyurethane foam (not shown in Fig 1) The two tray design separates the solar still into two chambers connected by the slot in the upper chamber The brine drain-off tube is soldered to the bottom of the upper tray (viz , in tilted position) and passes through the lower tray (via a stuffing box) The evaporation plate, i e , the upper tray, is covered by a thin black porous fabric (wick) The serpentine tube carrying the feedstock in the lower chamber is attached to the bottom of the upper tray and the feedstock exits the serpentine tube onto the upper tray via its slot (cf Figs 1 and 2) and is evenly distributed over the width of the wick by means of an overflow weir near the top of the upper tray The solar still module dimensions are listed Table 2

Solar simulator

The solar simulator consists of 16 halogen lamps (12 x 500 W and 4 x 300 W lamps), each fitted with a radiating screen of the same geometry which direct the radiation downward to the still The simulator is positioned parallel to the solar still and the lamp arrangement was verified experimentally to provide an essentially homogeneous radiation intensity on the still outer glazing surface A 10 mm thick double-walled polycarbonate sheet is positioned parallel between the simulator and still with a continuous stream of water flowing through it, in order to

filter any radiation above 2 6 μm emitted by the solar simulator The water absorbs the radiation in the 2 6 to 3 μm range, whereas the polycarbonate absorbs the radiation above 3 μm The temperature of the filter, viz , the polycarbonate sheet, is 18^{0}C at the lower end, water entrance, and 30^{0}C at the upper end, water exit Thus, its average temperature is below the average room temperature, 25 to 29 ^{0}C This setup insures that the radiation incident on the solar still is in the range between 0 4 to 2 6 μm (the UV component of the lamp radiation is negligible, since the lamp filament temperature is approx 2500 K)

External heat exchanger

The external heat exchanger was a standard laboratory glass condenser having a heat exchanger surface area of about 0 07 m^2 The heat exchange medium was mains water, entering with a temperature in the range of 15-18 ^{0}C and flowing countercurrently to the air stream exiting from the solar still's lower chamber It was sized for the estimated optimum operating conditions and therefore it was unable to cool the air stream vented to the ambient to room temperature, about 26 ^{0}C, for air mass flow rates in excess of 1 kgm^{-2}h^{-1}

Experimental conditions and procedure

The tilt angle of the solar still module and solar simulator was set at 20° throughout this study The solar radiation intensity, provided by the solar simulator, incident on the outer glazing surface was 630±39 Wm^{-2} The differential and cumulative yields from Separator I and II were measured automatically by a type PT 6 Satorius electric balance with an accuracy of ± 1 g The temperatures were measured with an accuracy of ± 1 °C using calibrated temperature sensors of the silicon base type KTY 11-2A. The absolute humidity of air in the vicinity of the slot was calculated from the mass and energy balances on the still A data acquisition system served to monitor and store the temperature data from the sixteen thermistors and to calculate differential and cumulative yields at variable time intervals It consisted of a PC with an A/D-D/A

46

converter card, electronic measuring and magnetic valve control unit, temperature sensors and a digital balance with a RS232C serial interface The data acquisition, control and analysis software were developed for the study

The experimental procedure for the performance testing was as follows

(1) the air and feedstock flow rates are defined and held constant,

(2) the temperatures at the following locations are monitored

air stream- upper chamber inlet, equally spaced probes in the direction of flow and above the slot,

lower chamber below the slot, equally spaced probes in the direction of flow and at the outlet,

saturated air stream exiting the still to the external condenser,

feedstock- lower chamber inlet,

upper chamber overflow weir and brine drain-off outlet,

(3) the distillation rate is determined by measuring the cumulative distillate during a specified time interval

5 RESULTS

The solar still performance was tested as a function of the air flow rate, which was varied in the range between 0 32 to 4 51 $kgm^{2}h^{1}$ The feedstock flow rate was maintained constant at 2 96 $kgm^{-2}h^{1}$ The solar still achieved steady-state, as evidenced by monitoring both air stream temperatures and the distillation rate, after approximately one hour of operation The maximum air stream temperature, in the range between 71 6 to 96 9 ^{0}C (inverse function of the air flow rate), was measured at the upper end of the solar still, in the vicinity of the slot (cf Table 3) It was determined that thermal energy recycle begins to take effect after about 30 minutes by comparing the continuously monitored air stream temperatures at the inlet to the upper chamber to that at the outlet from the lower chamber, viz , after about 30 minutes the latter exceeded the former The steady-state distillation rate was found to be of the order of 1 $kgm^{2}h^{1}$, except for relatively low air flow rate It is of interest to note, that if the air pump

remained in operation after the solar simulator was shut-off and the system was at steady-state, the still continued to produce distillate, albeit at a decreasing rate, for about another hour In other words, in spite of the relatively low thermal mass of the solar still module, thermal energy recycling is still capable of enhancing the yield after 'sunset', i e , after the solar simulator is shut-off

The steady-state temperatures, as measured by the 16 thermistors (cf Fig 1 for thermistor locations) are reported in Table 3 as a function of air flow rate As expected, temperature measured at a specific location varies inversely with the air flow rate, viz , it increases with decreasing air flow rate or increasing residence time within the still

Productivity as a function of air flow rate

The productivity, i e , distillation rate, as a function of air flow rates in the range from 0 32 to 4 51 $kgm^{-2}h^{-1}$ is reported in Table 4 in terms of primary (I), secondary (II), and total (Σ) The primary distillation rate refers to that condensed within the lower chamber during the thermal energy recycle process, but in fact contains a marginal amount of distillate (which is non-negligible when performing precise mass and energy balance calculations) condensed within the tubing connecting the lower chamber outlet to the exchnager The secondary distillation rate is that obtained by passing the saturated air stream exiting the solar still through an external condenser prior to venting to the ambient It is apparent from Table 4 that with regard to still productivity there exists an optimum range of air flow rates for the system under consideration, approximately between 1 and 3 $kgm^{-2}h^{-1}$ It is also observed that the ratio of secondary to primary product increases with increasing flow rate, i e , the primary decreases and the secondary increases with increasing air flow rate (cf Fig 3) The reason for optimum air flow rate will be discussed in the next section

6 DISCUSSION

Thermal energy analysis, utilizing mass and energy balances, of the solar still at steady-state as a function of air flow rate, for a constant feedstock flow rate of 2 96 kgh^{-1}, were performed in order to determine the sensitivity of a number of still parameters to changes in the rate of air flow The results of these analysis are reported in Table 5 and include the following (a) the mass flow rate of vapor through the system, (b) the mass and heat flow of both feedstock and brine drain-off, (c) heat flow in upper chamber and (d) heat flow in lower chamber In this analysis the temperature of the entering air stream and feedstock were assumed to be $\cong 26\ ^0C$, viz , room temperature, and an average value of 80% was assumed for the relative humidity of the entering air stream

The measured primary distillation rate (I) is a good approximation of the rate of condensation in the lower chamber but as mentioned previously it also contains that quantity of distillate condensed in the tubing connecting the outlet from the lower chamber to heat exchanger To enhance the precision of the mass and energy balances the flow rate of primary distillate exiting the lower chamber, m_I, was determined as the difference between the measured primary distillation rate and condensation rate of saturated air stream in the tubing between the lower chamber outlet and exchanger The latter is determined from the flow rate of bone dry air (BDA) in the following manner

$$m_I = I - m_{BDA}[M_v(\text{at } T_{I,out}) - M_v(\text{at } T_{X,in})], \qquad (6)$$

where M_v is in units of (kg vapor/kg BDA) The maximum mass flow rate of vapor carried by the air stream corresponds to that at maximum temperature and is given as

$$m_{v,max} = m_I + m_{BDA}[M_v(\text{at } T_{I,out})] \qquad (7)$$

The maximum rate of heat flow, q_{max}, is also achieved at T_{max} and if the flow rate of air and vapor is expressed in $kgm^{-2}s^{-1}$, q_{max} (in units of Wm^{-2}) is given by

$$q_{max} = c_a\, m_a\, T_{max} + m_{v\,max}\, H_{v\,max}, \qquad (8)$$

where c_a is the heat capacity of air in $Jkg^{-1}K^{-1}$ and $H_{v\,max}$ is the enthalpy of the vapor at T_{max} in units of Jkg^{-1}

It is apparent from Table 4 that the optimum performance of the solar still module is obtained for air flow rates in the range of 1 to 2 2 $kgm^{-2}h^{-1}$, which correspond to a total productivity rate of about 1 1 $kgm^{-2}h^{-1}$ In addition, it is observed from Table 5 (c) that within this range of air flow rates the amount of solar energy utilized, Q_u, decreases with decreasing air flow rate, whereas the average temperatures within the upper chamber increase with decreasing flow rate, cf Table 3 However, it is also observed from Table 5 that within this range of air flow rates, despite the decrease in Q_u with decreasing air flow rate, maximum values for primary distillation rate, m_I, total thermal energy recycle, q_{RT}, sum of thermal energy recycled directly to the upper chamber, q_R, and thermal energy released from the feedstock to the air stream in the upper chamber, $q_{released}$ occur for air flow rates between 1 02 and 1 24 $kgm^{-2}h^{-1}$ Thus, in this range of air flow rates the thermal energy recycle more than compensates for the decrease in solar energy efficiency, i e , the first effect or direct solar to thermal energy conversion

As a consequence of the above, it follows that in the range of 1 to 2 2 $kgm^{-2}h^{-1}$ air flow rates the mass flow rate of water vapor exiting the lower chamber will be a minimum in the range of air flow rates between 1 02 and 1 24 $kgm^{-2}h^{-1}$ and the air stream temperature, $T_{l,out}$, will be a maximum As a result, the cooling load for the external heat exchanger will be a minimum in this range of air flow rates

To demonstrate the heat flow processes occurring in the solar still module in this range of optimum performance a thermal energy flow diagram is presented in Fig 4 for an air flow rate of 1 24 $kgm^{-2}h^{-1}$ It is seen from this diagram that the main heat transfer processes determining the solar still performance are Q_u, q_R and q_{RT}

50

The decrease in the solar still performance for air flow rates below 1 $kgm^{2}h^{1}$ is the result of two factors (1) the increase in thermal energy losses from the upper chamber to the ambient, $q_{loss,amb}$, and (2) the overall heat transfer coefficient for thermal energy recycle, $U_{L,u}$, decreases rapidly with decreasing heat transfer coefficient for the gas film, h_g The latter is approximately proportional to the linear velocity of air stream (i e , the air and non-condensing water vapor) in the lower chamber Consequently, a possible design change to enhance the solar still performance would be to attain higher linear air velocities in the lower chamber by decreasing its cross-sectional area The downside of such a design change would be an increase in the pressure drop of the still system and a subsequent increase in parasitic energy consumption Since the present solar still design has a very low pressure drop there appears to be sufficient leeway for further reduction in the lower chamber cross-sectional area and we plan to study this effect in the future

Further development in the solar still design will be related to problems of scale-up, with the goal of arriving at a still design which is economically viable with regard to construction, operation and maintenance

7 CONCLUSIONS

The design and performance testing of a double glazed, air-blown, multiple-effect solar still with thermal energy recycle consisting of two chambers, upper evaporator and lower condenser, has been presented A considerable fraction of the latent heat of condensation is recycled for directly heating the evaporation plate and for preheating the feedstock and thereby enhancing the rate of the evaporation process

The heat transfer processes are based upon film condensation from a saturated air stream, which is characterized by a relatively high heat transfer coefficient, especially when operating at relatively high temperatures These high temperatures are achieved by operating the solar still

51

system at low air mass flow rates In addition, the heat transfer process is further enhanced by the increasing the air stream velocities in the lower (condensation) chamber

The optimum feedstock flow rate was found, based upon experimental results obtained utilizing a solar simulator with a constant radiation intensity of 630±39 Wm^{2}, to be in the range of 3 $kgm^{2}h^{1}$ This feedstock flow rate is sufficient to maintain the wick in the upper evaporation chamber completely wetted at even higher incident radiation intensities and thereby, higher evaporation rates

It was observed that the solar still performance was a mainly a function of the flow rate of the entering air stream In this study, the solar still operated under a constant feedstock flow rate of 2 96 $khm^{2}h^{1}$ and radiation intensity of 630±39 Wm^{2}, the optimum air flow rate was found to in the range of 1 02-1 24 $kgm^{2}h^{1}$, which corresponds to a maximum total productivity of 1 1 $kgm^{2}h^{1}$ The total productivity consists of about 0 9 $kgm^{2}h^{1}$ primary distillate (condensed within the lower chamber) and the remainder secondary distillate produced within the external condenser

The solar still system operates under a very low pressure drop, of the order of several Pa per m^2 of still area, for low (viz , optimum range) air flow rates This is a distinct advantage with regard to both still construction and parasitic energy requirements for air blowers, especially for large scale systems

The experimental results suggest that the solar still performance can be further enhanced by either decreasing the cross sectional flow area in the lower chamber and/or increasing the path length within the lower chamber of the still by the addition of baffles in order to achieve higher linear air velocities

In next generation of this solar still design, we will consider a number of modifications to simplify the still construction In addition, we plan to utilize the feedstock as the heat exchange medium (cooling stream) for the external condenser

52

Acknowledgment- This research was supported under Grant No TA-MOU-95-C15-050, US-Israel Cooperative Development Research Program, Office of Agriculture & Food Security, Center for Economic Growth, Bureau for Global Programs, Field Support and Research, USAID

NOMENCLATURE

A	still area (m^2)
c	heat capacity ($Jkg^{-1}K^{-1}$)
G	solar radiation (Wm^{-2})
H	enthalpy (Jkg^{-1})
h	heat transfer coefficient ($Wm^{-2}K^{-1}$)
M_v	vapor content of air stream (kg vapor/kg BDA)
m	mass flow rate ($kgm^{-2} h^{-1}$)
$m_{brine\ drain}$	mass flow rate of brine drain-off ($kgm^{-2}h^{-1}$)
Q_u	solar energy utilized (Wm^{-2})
q	thermal energy (Wm^{-2})
$q_{B\ loss}$	backside thermal energy losses (Wm^{-2})
$q_{brine\ drain}$	thermal energy in brine drain-off (Wm^{-2})
$q_{loss,amb}$	thermal energy loss from upper chamber to ambient (Wm^{-2})
q_{PR}	thermal energy utilized to preheat the feedstock (Wm^{-2})
q_R	thermal energy recycled directly to upper chamber (Wm^{-2})
$q_{released}$	thermal energy released by the preheated feedstock to the air stream (Wm^{-2})
q_{RT}	total thermal energy recycled (Wm^{-2})
T	temperature (^0C)
T_{dew}	dew point temperature of air stream exiting upper chamber and entering lower chamber (^0C)
U_{lw}	overall heat transfer coefficient from lower chamber to wick ($Wm^{-2}K^{-1}$)

Subscripts

a	air stream
abs	absorbed
amb	ambient
avg	average value
BDA	bone dry air
c	condensed water film
c,g	combined heat transfer coefficient
evap	evaporated
f	feedstock
g	gas film
I	primary distillate
II	secondary distillate
i	incident

in	stream entering chamber
l	lower chamber
m	central metal plate
max	maximum value
out	stream exiting chamber
r	reflected
sd	scale deposit
sep	vapor/liquid separator
t	serpentine tube
u	upper chamber
v	water vapor
w	wick
X	external heat exchanger/condenser

REFERENCES

Assouad, Y and Lavan, Z (1988) Solar desalination with latent heat recovery *J Solar Energy Engineering* **110**, 14-16

Delyannis, A and Delyannis, E E (1980) *Seawater and Desalting*, Vol 1 pp 67-70, Springer-Verlag, Berlin

Engelhardt, M , Kessling, W , Hauer, A and Scholkopf, W (1997) Solar thermal sea-water desalination Proceedings of the International Solar Energy Society, August 24-29, Taejon, Korea, in press

Kossinger, F , Jung, D and Sizeman, R (1993) Autonomous solar desalination plants with internal free convection *Proc ISES Solar World Congress*, August, Budapest Hungary, Vol 4, 331-336

Kudish, A I (1991) Water Desalination In *Solar Energy in Agriculture-Energy in World Agriculture*, Parker, B F (Ed), Vol 4, pp 255-294 Elsevier Science Publishers B V , Amsterdam

Malik, M A S , Tiwari, G N , Kumar, A and Sodha, M S (1982) *Solar Distillation*, Pergamon Press, Oxford, 175 pp

Mink, G Jakabos, D and Szekely, T (1988) Hungarian Patent, 201,714

Mink, G Aboabboud, M M and Karmazsin, E (1997a) Air-Blown Solar Still with Heat Recycling, *Solar Energy* (in press)

Mink, G , Aboabboud, M M , Horvath, L , Evseev, E and Kudish, A I (1997b) Design and performance of an air-blown, multiple-effect solar still with thermal energy recycle Proceedings of the International Solar Energy Society, August 24-29, Taejon, Korea, in press

Lobo, P C and Araujo, S R.D 1977 Design of a simple multi-effect basin-type solar still Proc Int'l Solar Energy Society Congress, New Delhi, p 2026

Rahim, N A. (1995) Utilization of forced condensing technique in moving film inclined solar still *Desalination* **101**, 255-262

Sodha, M S , Nayak, J K , Tiwari, G N and Kumar, A 1980 Double-basin solar still *Energy Conversion and Management* **20**, 23-31

Talbert, S G , Eibling, J A and Lof, G O G 1970 Manual on Solar Distillation of Saline Water, R&D Progress Report No 546, US Department of Interior, 263 pp

Thomas, D L , Guinn, G R and Thomason, B O (1990) Analysis of ventilated solar evaporator for concentrating dilute hazardous waste *Solar Energy* **45**, 101-104

54

Yeh, H M and Chen, L C (1985) Basin-type solar distillation with air flow through the still *Energy* **10**, 1237-1241

Yeh, H M and Chen, Z F (1994) Energy balances for upward-type, double-effect solar distillers with air flow through the second-effect unit *Energy* **19**, 619-626

55

List of Tables

Table 1 Overall heat transfer coefficient for thermal energy recycle U_{lw} as a function of temperature and the heat transfer coefficient for the gas film h_g for a wick thickness of 1 mm

Table 2 Dimension of solar still module

Table 3 The temperature profile of the solar still at steady-state as a function of air flow rate for a constant feedstock flow rate of 2 96 $kgm^{2}h^{1}$ The position of the 16 thermistors are as indicated in Fig 1 (numbered 0 to 16)

Table 4 Still productivity (I- primary distillate, II- secondary distillate, Σ- total distillate) as a function of air flow rate for a constant feedstock flow rate of 2 96 $kgm^{2}h^{1}$

Table 5 Mass and energy analysis of solar still at steady-state as a function of air flow rate for a constant feedstock flow rate of 2 96 $kgm^{2}h^{1}$ The mass and heat flows were normalized to unit still areas

(a) Mass flow rates of the water vapor through the solar still, (b) Mass and heat flow rates of feedstock/brine through the solar still, (c) Heat flows in upper evaporation chamber, (d) Heat flows in lower condenser chamber

Table 1 Overall heat transfer coefficient for thermal energy recycle U_{Lw} as a function of temperature and the heat transfer coefficient for the gas film h_g for a wick thickness of 1 mm

T, °C	90	85	80	75	70	65	60	55	50	45	40	35
$h_g = 80\ Wm^{2}K^{1}$ U_{Lw} ($Wm^{2}K^{1}$)	437	425	413	398	382	362	343	320	297	273	246	223
$h_g = 20\ Wm^{2}K^{1}$ U_{Lw} ($Wm^{2}K^{-1}$)	391 436*	358 393*	324 354*	290 315*	258 277*	225 240*	198 209*	169 177*	146 152*	124 128*	104 107*	88 90*
$h_g = 10\ Wm^{2}K^{1}$ U_{Lw} ($Wm^{2}K^{1}$)	342	292	251	213	180	150	126	104	87	72	59	49
$h_g = 5\ Wm^{2}K^{1}$ U_{Lw} ($Wm^{2}K^{1}$)	275	215	173	139	113	90	73	59	48	39	31	26

* for a wick thickness of 0 5 mm

Table 2 Dimension of solar still module

Double-glazing	10 mm thick double-walled polycarbonate sheet, L = 1 95 m, W = 0 6 m
Upper chamber	1 mm thick copper, L = 1 87 m, W = 0 545 m, H = 12 mm, rim width = 30 mm Spacing between the two chambers = 12 mm
Wick	0 3 mm thick black porous fabric, L = 1 85 m, W = 0 545 m, A = 1 m^2, weir height = 6 mm Spacing between textile and inner glazing = 12 mm It is assumed that the wick thickness is independent of water load
Lower chamber	1 mm thick copper, L = 1 9 m, W = 0 55 m, H = 25 mm, rim width = 30 mm
Serpentine tube	copper, L = 6 m, D_{inner} = 10 mm, D_{outer} = 12 mm, A = 0 20 m^2
Baffles	nine baffles soldered to the bottom of lower chamber, H = 12 mm for all baffles, L = 0 44 m for seven baffles, L = 0 36 m and 0 28 m for each of the remaining two baffles
Still casing	wood, L = 2 06 m, W = 0 7 m, H = 90 mm, bottom thickness = 10 mm, side thickness = 15 mm
Bottom and edge insulation	50 mm thick polyurethane foam, conductivity = 0 04 W $m^{-1}K^{-1}$

Table 3 The temperature profile of the solar still at steady-state as a function of air flow rate for a constant feedstock flow rate of 2 96 kgm^{2}h^{1} The position of the 16 thermistors are as indicated in Fig 1 (numbered 0 to 16)

Air Flow rate	T_a	UPPER CHAMBER					LOWER CHAMBER					$T_{I\,out}$	$T_{Sep,I}$	$T_{\chi,in}$	$T_{\chi,out}$	$T_{Brine\ drain}$
kgm^{2}h^{1}	T0 °C	T1 °C	T2 °C	T3 °C	T4 °C	T5 °C	T6 °C	T7 °C	T8 °C	T9 °C	T10 °C	T11 °C	T12 °C	T13 °C	T14 °C	T15 °C
4 51	26 0	51 2	65 6	72 2	71 3	71 6	71 3	70 6	69 9	66 0	56 0	56 0	54 9	54 6	35 4	48 7
3 27	26 4	54 0	71 1	76 4	75 9	76 6	76 7	75 9	75 1	71 1	59 6	59 6	58 1	57 8	36 0	51 5
2 21	26 3	57 5	77 1	81 3	81 2	82 1	82 1	81 6	80 7	77 0	63 1	63 1	60 9	60 4	35 0	54 5
1 76	26 1	59 1	80 1	83 7	83 7	84 7	84 8	84 3	83 5	79 9	64 4	64 4	62 0	61 3	34 1	55 7
1 24	26 6	62 6	84 6	87 4	87 6	88 4	88 5	88 4	87 5	84 4	67 5	67 5	64 1	63 0	32 1	58 4
1 02	26 2	64 9	87 4	89 8	89 8	90 7	90 7	90 7	90 0	87 2	69 9	69 9	65 6	64 1	28 6	60 4
0 58	26 1	67 6	91 9	93 6	93 6	94 4	94 2	94 5	94 0	91 7	68 2	68 2	60 7	57 1	21 9	61 9
0 32	25 8	68 6	95 1	96 3	96 2	97 0	96 9	97 4	96 9	94 9	52 5	48 9	34 0	30 4	24 1	62 4

Table 4 Still productivity (I- primary distillate, II- secondary distillate, Σ- total distillate) as a function of air flow rate for a constant feedstock flow rate of 2 96 $kgm^{2}h^{1}$

Air Flow Rate ($kgm^{2}h^{1}$)	I ($kgm^{2}h^{1}$)	II ($kgm^{2}h^{1}$)	Σ ($kgm^{2}h^{1}$)
4 51	0 65	0 32	0 97
3 27	0 75	0 29	1 03
2 21	0 84	0 27	1 11
1 76	0 87	0 20	1 07
1 24	0 96	0 15	1 11
1 02	0 97	0 13	1 10
0 58	0 93	0 04	0 97
0 32	0 68	0 01	0 69

Table 5 Mass and energy analysis of solar still at steady-state as a function of air flow rate for a constant feedstock flow rate of 2 96 $kgm^{-2}h^{-1}$ The mass and heat flows were normalized to unit still areas

(a) Mass flow rates of the water vapor through the solar still

Upper Chamber		Lower Chamber		Tubing			Heat exchanger	
m_a $kgm^{-2}h^{-1}$	$m_{v\,u,in}$ $kgm^{-2}h^{-1}$	m_{evap} $kgm^{-2}h^{-1}$	$m_{v\,max}$ $kgm^{-2}h^{-1}$	m_I $kgm^{-2}h^{-1}$	$m_{v\,l,out}$ $kgm^{-2}h^{-1}$	m_{II} $kgm^{-2}h^{-1}$	$m_{v,X,in}$ $kgm^{-2}h^{-1}$	$m_{v\,X,out}$ $kgm^{-2}h^{-1}$
4 51	0 078	1 082	1 160	0 614	0 546	0 036	0 510	0 190
3 27	0 056	1 136	1 192	0 703	0 489	0 047	0 442	0 152
2 21	0 038	1 149	1 187	0 781	0 406	0 059	0 347	0 077
1 76	0 030	1 131	1 161	0 812	0 349	0 058	0 291	0 091
1 24	0 021	1 166	1 187	0 891	0 296	0 069	0 227	0 077
1 02	0 018	1 151	1 169	0 887	0 282	0 073	0 209	0 077
0 58	0 010	0 996	1 006	0 861	0 145	0 069	0 076	0 036
0 32	0 006	0 683	0 689	0 657	0 032	0 023	0 009	0

(b) Mass and heat flow rates of feedstock/brine through the solar still

Lower Chamber				Upper Chamber					
m_a $kgm^{-2}h^{-1}$	T_{max} °C	$m_{f,in}$ $kgm^{-2}h^{-1}$	$q_{f\,l,in}$ at T_a Wm^{-2}	q_{PR} Wm^{-2}	$q_{f\,l,out}$ at T_{max} Wm^{-2}	$T_{Brine\ drain}$ °C	$m_{Brine\ drain}$ $kgm^{-2}h^{-1}$	$q_{Brine\ drain}$ Wm^{-2}	$q_{released}$ Wm^{-2}
4 51	71 6	2 96	90	156	246	48 7	1 878	106	139
3 27	76 7	2 96	90	174	264	51 5	1 824	109	155
2 21	8 21	2 96	90	193	283	54 5	1 811	115	168
1 76	84 8	2 96	90	202	292	55 7	1 829	118	174
1 24	88 5	2 96	90	215	305	58 4	1 794	122	183
1 02	90 7	2 96	90	222	312	60 4	1 809	127	185
0 58	94 2	2 96	90	234	324	61 9	1 964	141	183
0 32	96 9	2 96	90	245	334	62 4	2 277	164	170

(c) Heat flows in upper evaporation chamber

m_a kgm^{2}h^{1}	$q_{a,u,in}$ Wm^{2}	q_R Wm^{2}	$q_{released}$ Wm^{2}	Q_U Wm^{2}	q_{max} Wm^{2}	T_{max} °C	T_{dew} °C
4 51	110	216	139	470	935	71 6	68 7
3 27	80	256	155	451	942	76 7	74 2
2 21	54	285	168	415	922	82 1	79 8
1 76	43	296	174	383	896	84 8	82 3
1 24	30	330	183	363	906	88 5	86 4
1 02	25	316	185	363	889	90 7	88 5
0 58	14	289	183	274	760	94 2	91 7
0 32	9	154	170	187	520	96 9	93 0

(d) Heat flows in lower condenser chamber

m_a kgm^{2}h^{1}	T_{max} °C	T_{dew} °C	q_{max} Wm^{2}	$q_{l,out}$ Wm^{2}	q_I Wm^{2}	$q_{B\ loss}$ Wm^{2}	q_{RT} Wm^{2}	q_{PR} Wm^{2}	q_R Wm^{2}
4 51	71 6	68 7	935	491	40	33	371	156	215
3 27	76 7	74 2	942	426	50	36	430	174	256
2 21	82 1	79 8	922	345	58	41	478	193	285
1 76	84 8	82 3	896	294	61	43	498	202	296
1 24	88 5	86 4	906	245	70	46	545	215	330
1 02	90 7	88 5	889	231	72	48	538	222	354
0 58	94 2	91 7	760	119	74	50	571	234	316
0 32	96 9	93 0	520	60	42	50	417	245	152

Note Refer to the nomenclature for definition of symbols

List of Figures

Fig 1 A schematic diagram of the experimental solar still set-up The location of the temperature probes, thermistors are indicated by numbers 0 to 15

Fig 2 A schematic diagram of the lower condenser chamber, showing the serpentine tube through which the feedstock flows and the baffles

Fig 3 Productivity (yield) as a function of air flow rate for a constant feedstock flow rate of 2 96 $kgm^{2}h^{1}$ I is the primary distillate, II is the secondary distillate and Σ is the total distillate

Fig 4 Thermal energy flow diagram calculated by means of the mass and energy balances on the solar still for an air flow rate of 1 24 $kgm^{2}h^{1}$ and a feedstock flow rate of 2 96 $kgm^{2}h^{1}$

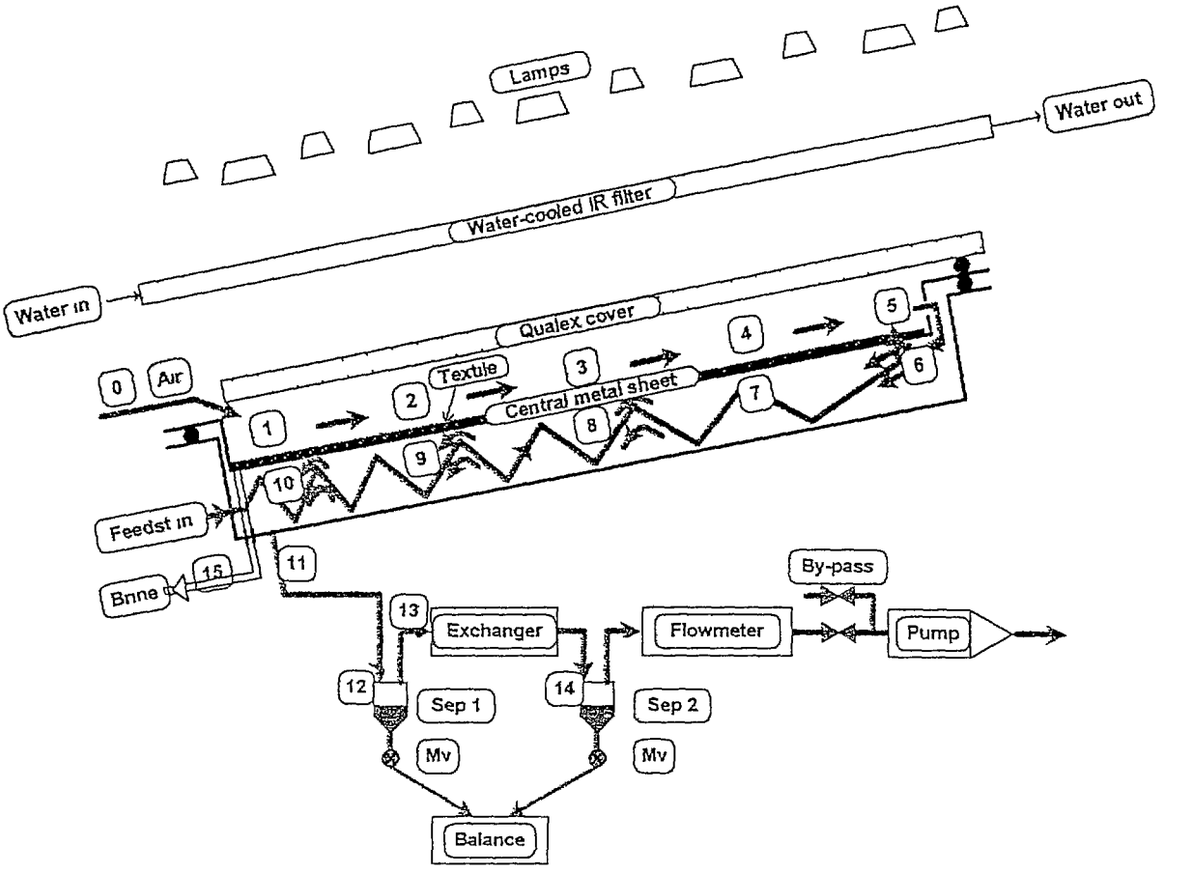

Fig 1 A schematic diagram of the experimental solar still set-up The location of the temperature probes, thermistors are indicated by numbers 0 to 15

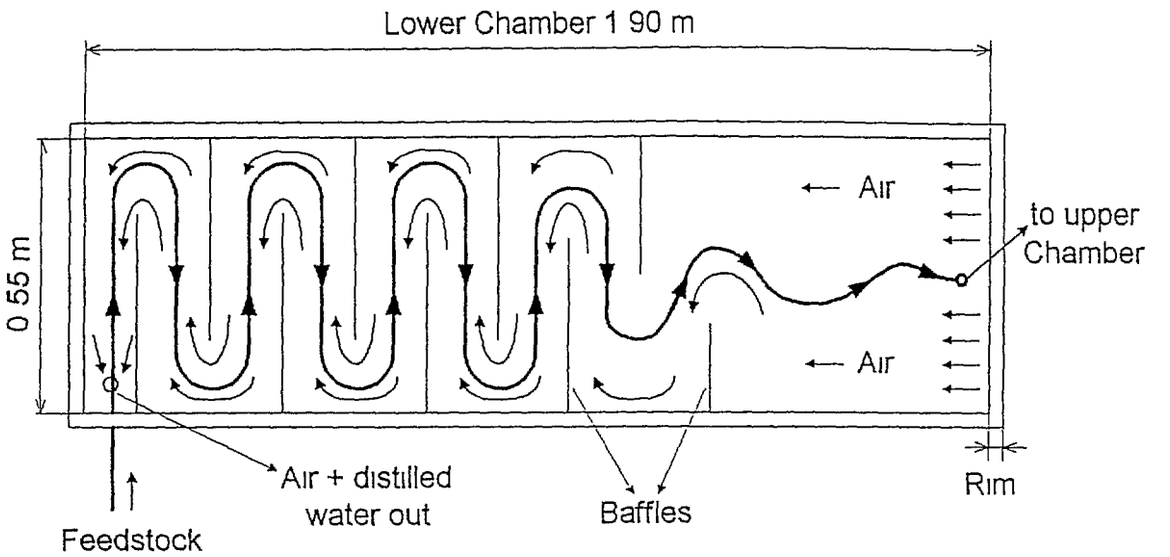

Fig 2 A schematic diagram of the lower condenser chamber, showing the serpentine tube through which the feedstock flows and the baffles

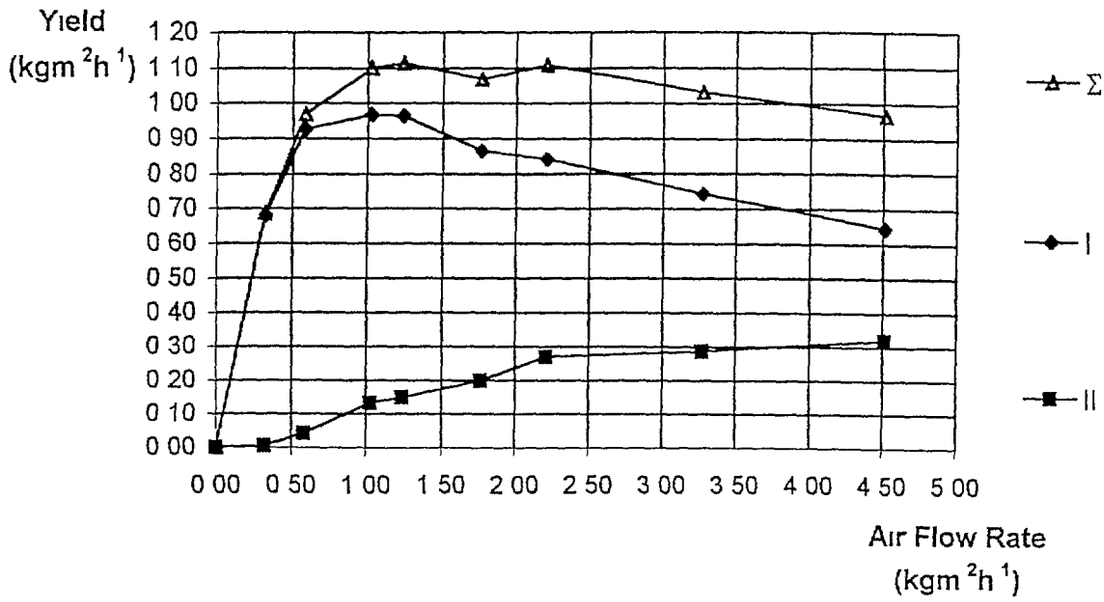

Fig 3 Productivity (yield) as a function of air flow rate for a constant feedstock flow rate of 2 96 kgm ^{2}h ^{1} I is the primary distillate, II is the secondary distillate and Σ is the total distillate

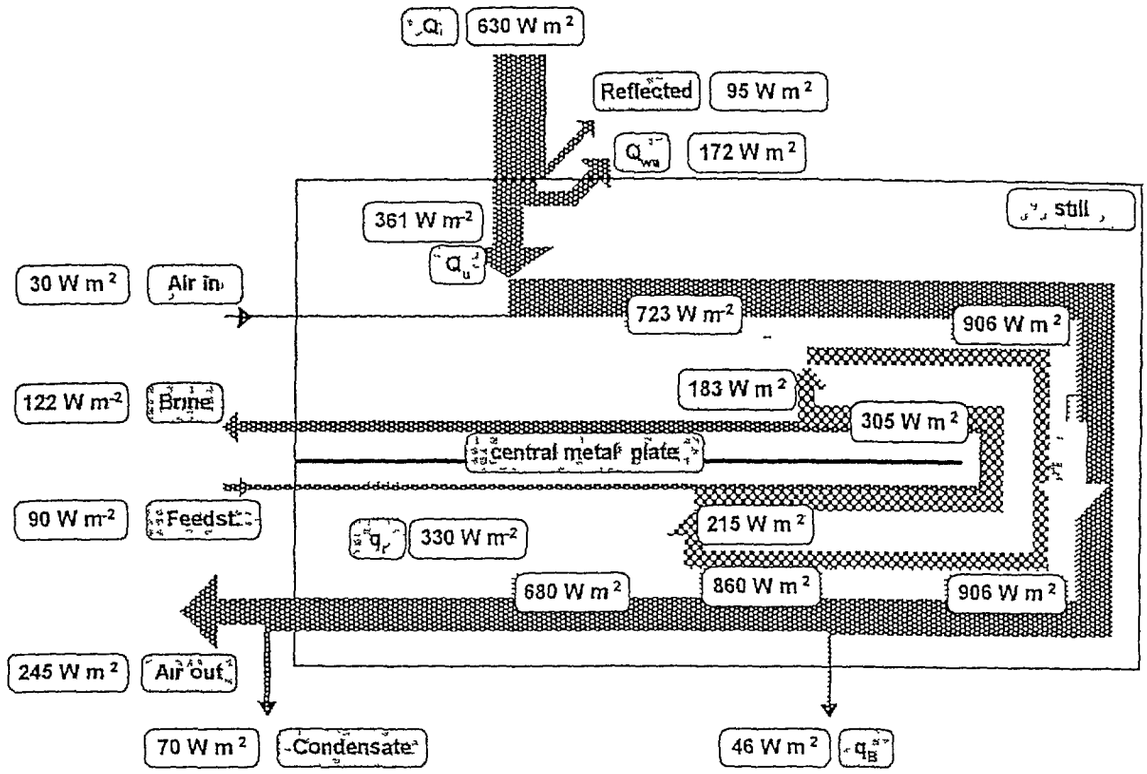

Fig 4 Thermal energy flow diagram calculated by means of the mass and energy balances on the solar still for an air flow rate of 1 24 kgm^{2}h^{1} and a feedstock flow rate of 2 96 kgm^{2}h^{1}